

Reaction to fire of an intumescent epoxy resin: Protection mechanisms and synergy

Caroline Gérard, Gaëlle Fontaine, Séverine Bellayer, Serge Bourbigot

▶ **To cite this version:**

Caroline Gérard, Gaëlle Fontaine, Séverine Bellayer, Serge Bourbigot. Reaction to fire of an intumescent epoxy resin: Protection mechanisms and synergy. Polymer Degradation and Stability, 2012, 97 (8), pp.1366-1386. 10.1016/j.polymdegradstab.2012.05.025 . hal-02090047

HAL Id: hal-02090047
https://hal.univ-lille.fr/hal-02090047

Submitted on 4 Apr 2019

HAL is a multi-disciplinary open access archive for the deposit and dissemination of scientific research documents, whether they are published or not. The documents may come from teaching and research institutions in France or abroad, or from public or private research centers.

L'archive ouverte pluridisciplinaire **HAL**, est destinée au dépôt et à la diffusion de documents scientifiques de niveau recherche, publiés ou non, émanant des établissements d'enseignement et de recherche français ou étrangers, des laboratoires publics ou privés.

Polymer Degradation and Stability xxx (2012) 1–21

Contents lists available at SciVerse ScienceDirect

Polymer Degradation and Stability

journal homepage: www.elsevier.com/locate/polydegstab

Reaction to fire of an intumescent epoxy resin: Protection mechanisms and synergy

Caroline Gérard [a,b,c,d], Gaëlle Fontaine [a,b,c,d], Séverine Bellayer [a,b,c,d], Serge Bourbigot [a,b,c,d,*]

[a] Univ Lille Nord de France, F-5900 Lille, France
[b] ENSCL, ISP-UMET, F-59652 Villeneuve d'Ascq, France
[c] USTL, ISP-UMET, F-59655 Villeneuve d'Ascq, France
[d] CNRS, UMR 8207, F-59652 Villeneuve d'Ascq, France

ARTICLE INFO

Article history:
Received 2 March 2012
Accepted 21 May 2012
Available online xxx

Keywords:
Epoxy
Intumescence
Synergy
Flame retardancy
POSS

ABSTRACT

This study investigates the effects of the incorporation of nanoparticles on the reaction to fire of an epoxy resin containing a conventional intumescent flame retardant. Two types of nanoparticles are considered: OctaMethylOligomericSilsesquioxanes (OMPOSS) and Carbon NanoTubes (CNTs). The combination of an intumescent phosphorus-based flame-retardant (APP) and CNTs provides no enhancement of the reaction to fire of this system. In contrast, using OMPOSS in combination with APP provides a large synergistic effect via an intumescence phenomenon. The study of the thermal degradation of these systems shows that the interactions between these fillers modify the viscosity of the degraded matrix. The trapping of degradation gases is enhanced in the case of APP/OMPOSS, which results in the creation of an intumescent protective layer earlier than with the reference system containing APP alone. Furthermore, the presence of OMPOSS permits the creation of silicophosphates which reinforce the residue. In contrast, the residue of the formulation containing carbon nanotubes is excessively stiff and it cracks during combustion, hindering the proper formation of the protective layer.

© 2012 Elsevier Ltd. All rights reserved.

1. Introduction

Since the development of polymer industry in the 20th century, plastics have spread to many fields of our everyday life. Among them, thermoset epoxy resins have been considerably developed since their first synthesis in 1930's. One of the current applications of epoxy resins is the design of structural parts in the automotive or aeronautic industry. This use is especially growing since these materials provide many advantages (e.g. lighter structure).

However, the numerous advantages of polymers should not hide one of their major drawbacks: their high flammability. Polymers are usually organic materials, and as such, they produce volatile combustibles when submitted to a heat source. If suitable conditions are fulfilled, this can result in the burning of the material and of its surrounding. This hazard is especially serious for aircraft, as people cannot escape fire during a flight. Indeed, in-flight fires and post-crash fires account for 20% of the fatalities resulting from airplane accidents [1]. Furthermore, in case of ignition, polymeric materials do not only fuel the fire, but they also release gases and smokes, some of them being toxic, which incapacitate passengers or make them panic because of a reduced visibility. Special effort is therefore required for increasing the fire safety in aircraft.

Nanoparticles build a recent class of fillers and their incorporation in polymers has attracted much interest in the last ten years. Indeed, compared to conventional fillers, they are incorporated at low loadings. This enables the enhancement of some properties, including the reaction to fire in some cases, without degrading others (e.g. mechanical properties). In contrast to thermoplastics, there are few references in the literature about the use of nanofillers as flame retardants in epoxy resins. There is therefore almost no information about their potential for enhancing the reaction to fire of thermosets. Furthermore, they may be part of an already flame-retarded formulation and interact with other fillers.

In a previous article [2], we reported different effects between a conventional flame retardant (ammonium polyphosphate, APP) and two types of nanoparticles in a model epoxy resin. The first of these nanofillers is OctaMethylOligomericSilsesquioxanes (OMPOSS), whereas the second is carbon nanotubes (CNTs). The incorporation of CNTs along with APP leads to an antagonism in terms of mass-loss calorimetry, while the use of OMPOSS with APP leads to a synergy. Moderate effects were identified by

* Corresponding author. ENSCL, ISP-UMET, BP 90108, F-59652 Villeneuve d'Ascq, France. Tel.: +33 (0)3 20 43 48 88; fax: +33 (0)3 20 43 65 84.
E-mail address: serge.bourbigot@ensc-lille.fr (S. Bourbigot).

0141-3910/$ – see front matter © 2012 Elsevier Ltd. All rights reserved.
doi:10.1016/j.polymdegradstab.2012.05.025

Please cite this article in press as: Gérard C, et al., Reaction to fire of an intumescent epoxy resin: Protection mechanisms and synergy, Polymer Degradation and Stability (2012), doi:10.1016/j.polymdegradstab.2012.05.025

thermogravimetric analysis, as well as by pyrolysis combustion flow calorimetry. However, the qualitative observation of the residual char showed different structures for the three formulations and the modified reaction to fire was attributed mostly to a physical effect. In this article, we aim at identifying the parameters influencing the reaction to fire of these formulations and elucidate the protection mechanisms. A systematic study is implemented in order to address to key issues: is the epoxy matrix modified by the presence of the different fillers? What are the main mechanisms explaining the phenomena observed during burning? First, the epoxy matrix will be characterized in terms of glass transition temperature, conversion degree, morphology and thermal conductivity. Then, the protection mechanisms will be investigated: the composition and appearance of the residues during combustion will be detailed. Finally, the dynamic evolution of the systems will be considered in terms of viscosity, temperature in the samples and occurrence of intumescence.

2. Experimental

2.1. Materials

Unless otherwise stated, all materials were obtained from commercial suppliers and used without further purification. Epoxy prepolymer (Bisphenol-A diglycidylether, Epoxy Equivalent Weight = 172–176) and the hardener diethylenetriamine (DETA, 99%) were supplied by Sigma–Aldrich. OMPOSS were purchased from Hybrid Plastics (MS0830, >97% purity). CNT were supplied by Nanocyl (Nanocyl 7000, 90% purity). APP was supplied by Clariant (AP422). Epoxy prepolymer was heated at 50 °C for 24 h in order to avoid crystallization before use.

2.2. Processing

Fillers were mechanically mixed with epoxy prepolymer at 1600 rpm for 20 min at room temperature (stirrer 94412 from Fischer Scientific). The stirrer was equipped with a disk-shaped tool and the mixing was carried out in 250 mL Nalgene containers. Batches of 80 g were prepared. The mixture was then sonicated for 1 h (100 W, 50 kHz, 50 °C) in a heated ultrasonic bath. After cooling down at room temperature, the amine hardener was mechanically incorporated in the mixture at 200 rpm for 5 min with the same stirrer as in the initial step. The mixture was then poured into aluminium moulds coated with a silicon-based mould release agent and degassed at room temperature for 10 min. The samples were then cured in a ventilated oven according to the following schedule: 30 min at 30 °C, 30 min at 40 °C and 1 h at 50 °C. The compositions of the formulations used in this work are described in Table 1. The prepolymer and the hardener are in stoichiometric ratio.

2.3. Glass transition temperature

Differential scanning calorimetry (DSC) was used to investigate the influence of fillers on the glass transition temperature of the studied epoxy samples. A Q100 DSC device from TA Instruments was used. The analysis was divided in 2 cycles: the first one removes the thermal history of the material and the second one is aimed at measuring the glass transition temperature. The samples were heated between −50 °C and 200 °C at 20 °C/min under a 50 mL/min nitrogen flow. The samples (5 mg) are enclosed in aluminium pans. The error margins for calculated glass transition temperatures lie around 2 °C.

Table 1
Composition of the formulations.

Formulation name	Epoxy (wt.%)	APP (wt.%)	CNT (wt.%)	OMPOSS (wt.%)
Virgin epoxy	100	–	–	–
Epoxy_OMPOSS-5	95	–	–	5
Epoxy_APP-5	95	5	–	–
Epoxy_APP-4.5_CNT-0.5	95	4.5	0.5	–
Epoxy_APP-4_OMPOSS-1	95	4	–	1

2.4. Conversion degree

Infrared spectra were recorded between 500 and 4000 cm^{-1} on a Nicolet 400D spectrometer equipped with a mono-reflexion ATR unit (Dura SamplIR II, SensIR, diamond crystal). In order to minimize the signal/background ratio, spectra result from 32 scans with a 4 cm^{-1} resolution. Omnic software was used for the processing of the interferograms and the spectra. The aforementioned spectrometer was equipped with a heating ATR unit (GladiATR, Pike Technologies) in order to follow the conversion degree in real time.

2.5. Morphology

Depending on the size of the fillers, Scanning Electron Microscopy (SEM) and Transmission Electron Microscopy (TEM) were used. For SEM, the samples were analysed with a Hitachi S4700 microscope. All samples were ultra microtomed at room temperature for surfacing. Secondary electron SEM images of composites were obtained at 6 kV, 10 μA.

For TEM, the samples were ultra microtomed with a diamond knife on a Leica ultracut UCT microtome, at room temperature, to give sections with nominal thickness of 70 nm. Sections were transferred to Cu grids of 400 meshes. Bright-field TEM images of composites were obtained at 200 kV under low dose conditions with a FEI TECNAI 62 20 electron microscope, using a Gatan CCD camera. Low magnification images were taken at 17,000× and high-magnification images were taken at 80,000×.

2.6. Thermal conductivity

The thermal conductivity of nanocomposites was measured by a Hot Disk thermal analyser (TPS2500, Sweden), which was based upon the transient plane source method. This apparatus was equipped with a heating furnace controlled by the Hot Disk software. The dimension of bulk specimens is 20 × 15 × 4 mm^3 with the sensor placed between two similar plates of materials. The sensor supplied a heat pulse between 0.01 W and 0.04 W for 40–160 s to the sample (depending on the sample) and recorded relevant temperature.

2.7. Fire testing and specific instrumentation

The Fire Testing Technology Mass Loss Calorimeter was used to perform measurements (reaction to fire) on samples following the procedure defined in ASTM E 906. Our procedure involved exposing specimens having a disk shape with a 77 mm diameter and 2.5 mm thickness in horizontal orientation. Specimens were wrapped in aluminium foil leaving the upper surface exposed to the heater and placed on a ceramic backing board at a distance of 25 mm from cone base (or 35 mm when the expansion is measured). External heat flux of 35 kW/m^2 was used for running the experiments. This flux corresponds to common heat flux in a mild fire scenario. Heat release rate (HRR) is measured as a function of time and it is reproducible to within 10%. Minimum three tests were carried out on each material.

Please cite this article in press as: Gérard C, et al., Reaction to fire of an intumescent epoxy resin: Protection mechanisms and synergy, Polymer Degradation and Stability (2012), doi:10.1016/j.polymdegradstab.2012.05.025

Intumescent samples are characterized by the formation of an insulating layer that forms on top of the sample during their burning. During mass-loss calorimeter experiments, K-type thermocouples were embedded in the samples at three different locations. This setting permits to evaluate the temperature gradients in the burning polymer.

In order to measure the swelling of intumescent samples during mass-loss calorimetry and link it to other parameters, the development of the char was monitored by an infrared camera. The obtained imaged were then processed via an image analysis software and the relative swelling was calculated.

2.8. Solid-state Nuclear Magnetic Resonance (NMR)

Mass-loss calorimeter experiments were stopped at characteristic times of the combustion and the composition of the residues was studied by solid-state NMR.

^{31}P NMR analyses are carried out on a Bruker Avance II 400 spectrometer with a 4 mm probe. The Larmor frequency is 40.5 MHz (9.4 T). Measurements are performed with ^{1}H dipolar decoupling at 10 kHz in MAS (Magic Angle Spinning) conditions. 120 s delay was used between two pulses. Phosphoric acid (H_3PO_4) in aqueous solution (85%) was used as a reference.

^{29}Si NMR analyses are carried out on the same spectrometer equipped with a 7 mm probe. Measurements are performed with cross-polarization and ^{1}H dipolar decoupling at 5 kHz in MAS conditions. Contact time was set at 1 ms and the delay between pulses was 5 s. Tetramethylsilane ($Si(CH_3)_4$) was used as a reference.

^{13}C NMR analyses are carried out on the same spectrometer as above and equipped with a 4 mm probe. Measurements are performed with cross-polarization and ^{1}H dipolar decoupling at 10 kHz or 12.5 kHz in MAS conditions. Contact time was set at 1 ms and the delay between pulses was 5 s. Tetramethylsilane ($Si(CH_3)_4$) was used as a reference.

2.9. Rheology

A thermal scanning rheometer Rheometric Scientific ARES-20A, in a parallel plate configuration was used to measure the apparent viscosity of the formulations during degradation. Sample pellets (thickness = 1 mm) are positioned between the two plates. Testing is carried out using a "Dynamic Temperature Ramp Test" with a heating rate of 10 °C/min in the range 25–500 °C, a strain of 1% and a constant normal force of 100 N (200 Pa).

2.10. Digital microscopy

Digital microscopes are a variation of a traditional optical microscope that uses optics and a charge-coupled device (CCD) camera to output a digital image to a monitor. In our case, the microscope enables to get a clear view of residues obtained after burning thanks to the high depth of field. Images of chars were taken with a VHX-1000 microscope (Keyence) at 30× magnifications and stitched together in order to get a clear image of the whole char.

2.11. Electron-probe micro-analysis (EPMA)

Electron probe microanalysis (EPMA) is an analytical technique that is used to establish the composition of small areas on specimens. EPMA is one of several particle-beam techniques. A beam of accelerated electrons is focused on the surface of a specimen using a series of electromagnetic lenses, and these energetic electrons produce characteristic X-rays within a small volume (typically 1 to 9 cubic microns) of the specimen. The characteristic X-rays are detected at particular wavelengths, and their intensities are measured to determine concentrations. All elements (except H, He, and Li) can be detected because each element has a specific set of X-rays that it emits. This analytical technique has a high spatial resolution and sensitivity. Additionally, the electron microprobe be used as a scanning electron microscope and obtain highly magnified secondary- and back scattered-electron images of a sample.

In this article, the samples were characterized with a Cameca SX100 electron probe micro analyser with four wavelength dispersive X-ray spectrometers (WDS), which allows the performance of microscopic and elemental analyses.

Previously to the EPMA study, the sample was carbon coated with a Bal-Tec SCD005 sputter coater. Back scattered electrons (BSE) images were obtained at 15 kV, 10 nA. Si X-ray profile was carried out at 15 kV, 15 nA. A TAP (Thallium acid phthalate, $C_8H_5O_4Tl$) crystal was used to detect the Si Kα X-ray.

3. Results and discussion

3.1. Glass transition temperature

DSC was used for the evaluation of the glass transition temperature (T_g). It shows that the T_g is not greatly affected by the incorporation of the fillers (Table 2). Indeed, it varies between 130 and 136 °C, with error margins lying around 2 °C.

3.2. Conversion degree

In order to further study the possible modifications of the epoxy matrix induced by the incorporation of fillers, the curing kinetics was assessed by using a heating ATR-IR spectrometer.

Fig. 1 shows the conversion degree as a function of time for the five epoxy formulations. During the first curing step at 30 °C, all formulations begin to cure and Virgin epoxy, Epoxy_APP-5 and Epoxy_APP-4_OMPOSS-1 exhibit the same rate of curing. It seems therefore that APP does not affect the curing rate of epoxy. It is lower for the sample containing OMPOSS alone. The sample containing both APP and CNTs also has a lower curing rate at shorter times. At the end, the crosslinking degrees are very similar for Virgin epoxy, Epoxy_OMPOSS-5 and Epoxy_APP-4_OMPOSS-1. They are slightly lower for Epoxy_APP-5 and Epoxy_APP-4.5_CNT-0.5. Therefore, the curing rate is lower for Epoxy_OMPOSS-5 at the beginning, but the effect is reduced thereafter and the final crosslinking degree is close to that of virgin epoxy. In contrast, Epoxy_APP-5 behaves like virgin epoxy at the beginning and has a lower final crosslinking degree. Finally, Epoxy_APP-4.5_CNT-0.5 is less reactive during the whole experiment.

These results are consistent with the literature, even if no reference was found on the reactivity of epoxy containing APP. There are however many reports on the effects of nanoparticles on the curing process of epoxies. In our case, POSS incorporated alone in the matrix slows down the curing during the step at 30 °C. Zhang et al. [3] have also observed a lower curing rate at the beginning of the curing of epoxy containing 10 wt.% octaaminopropylPOSS.

Table 2
Glass transition temperature (T_g) of the different formulations.

Formulation	T_g (°C)
Virgin epoxy	132
Epoxy_OMPOSS-5	132
Epoxy_APP-5	136
Epoxy_APP-4.5_CNT-0.5	130
Epoxy_APP-4_OMPOSS-1	133

Please cite this article in press as: Gérard C, et al., Reaction to fire of an intumescent epoxy resin: Protection mechanisms and synergy, Polymer Degradation and Stability (2012), doi:10.1016/j.polymdegradstab.2012.05.025

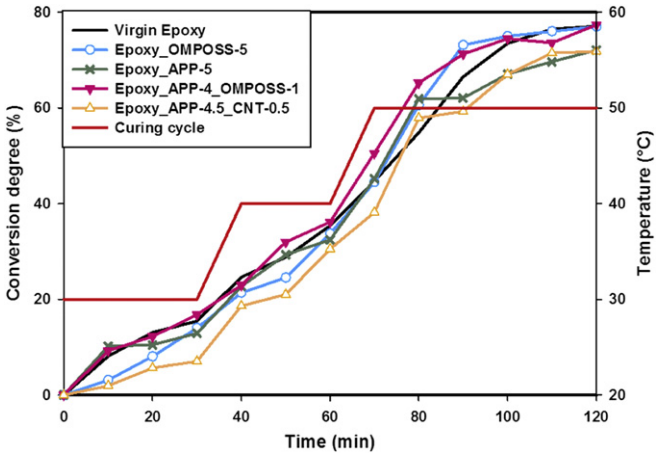


Fig. 1. Conversion degree as a function of time for the five formulations.

Concerning CNTs, our results suggest a retardation of the curing during the whole experiment. Allaoui et al. [4] have reviewed literature on epoxy containing CNTs: although accelerated cure in the early stage is reported in many cases, no effect or even retardation occur in another one. The presence of residual catalysts in CNTs is frequently identified as the main parameter accelerating the curing. In our case, it can be suggested that the agglomeration of CNTs into bundles limits this catalytic effect.

3.3. Morphology

It has been shown in the literature that the dispersion of fillers in a polymer matrix can influence the reaction to fire of polymers [5]. Therefore, epoxy samples were characterized by electronic microscopies.

Depending on the filler size, the five formulations were studied by Scanning Electron Microscopy (SEM) and some of them by Transmission Electron Microscopy (TEM). In fact, APP is a micrometric-sized filler with an average diameter of 15 μm. Therefore, SEM is the best method for the observation of this filler in the matrix. In contrast, nanofillers such as POSS and carbon nanotubes should be observed by TEM. Two parameters were particularly observed: the homogeneity of the dispersion in the whole matrix and the size of aggregates if present.

Fig. 2a shows the unfilled resin, observed in order to study the texture of the resin itself. It reveals that there is no specific appearance of the resin. Small particles are distinguished at the surface of the specimen, but they are likely resin shards produced during the preparation of the sample or dust particles.

The sample containing 5 wt.% OMPOSS reveals that POSS appear as small rods, some of them being individualized (Fig. 3). However, the quantity of POSS observed by TEM seems low compared to the theoretical content. It is because of the existence of big aggregates as shown by SEM (Fig. 2b).

The dispersion of APP was then examined (Fig. 2c). SEM pictures show that APP is homogeneously dispersed in the matrix. The particles are also individualized, as their size lie around 20 μm (mean particle size of APP is about 15–20 μm). The white lines are attributed to micro-fractures occurring during the preparation of the samples and initiated by APP agglomerates which act as stress concentration centres.

Combinations between micro- and nanofillers were then studied. First, the sample containing APP and OMPOSS was observed (Fig. 2d). In this case, SEM is used to evaluate the homogeneity of the dispersion. We can therefore observe that the dispersion of APP in epoxy in the presence of POSS is very similar to that of APP alone. Very small particles with diameter of a few microns are evenly dispersed in the matrix. A closer look on this sample by TEM shows that they are POSS or grinded APP particles (Fig. 4). Indeed, the morphology of the sample containing POSS alone has already been studied and discussed above and the hypothesis that the aggregates observed on Fig. 4 is supported by these previous observations of Epoxy_OMPOSS-5. The dispersion of POSS in the APP_OMPOSS-5 formulation is similar to that of OMPOSS alone. Small agglomerates (mean diameter: 0.5–1 μm) are evenly distributed in the whole sample.

Finally, the morphology of samples containing APP and CNTs was characterized. SEM pictures show that APP is homogeneously dispersed in the matrix, similarly to the sample containing APP alone (Fig. 2e and f). Areas with different texture (red arrows) are identified as CNT-rich areas (from the experience of the lab), as shown by larger magnifications. CNTs are not well dispersed in the matrix: some areas are completely free of them. Furthermore, holes in the matrix can be seen. They are likely due to the increase of

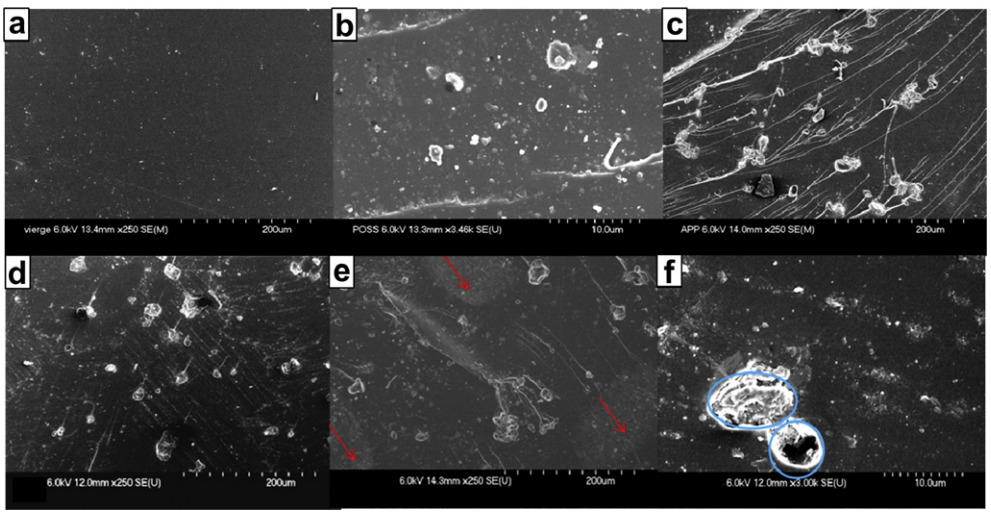


Fig. 2. SEM images of Virgin epoxy (a), Epoxy_OMPOSS-5 (b), Epoxy_APP-5 (c), Epoxy_APP-4_OMPOSS-1 (d), Epoxy_APP-4.5_CNT-0.5 (e and f – red arrows: CNT-rich area, blue circles: holes). (For interpretation of the references to colour in this figure legend, the reader is referred to the web version of this article.)

Please cite this article in press as: Gérard C, et al., Reaction to fire of an intumescent epoxy resin: Protection mechanisms and synergy, Polymer Degradation and Stability (2012), doi:10.1016/j.polymdegradstab.2012.05.025

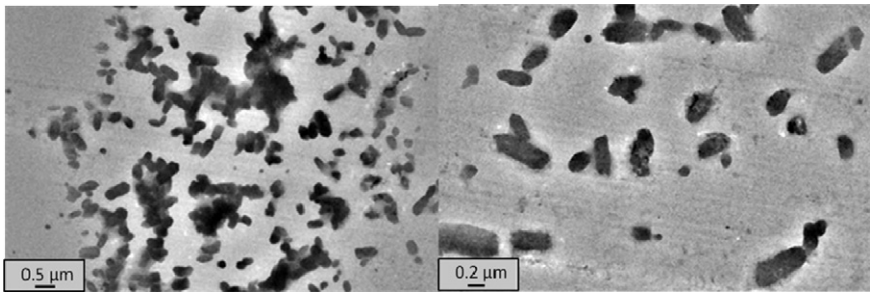


Fig. 3. TEM images of Epoxy_OMPOSS-5.

viscosity of the uncured material (due to the presence of CNTs), which does not permit the easy release of gases produced during curing (blue circles).

A closer look on the dispersion of CNTs in the matrix is given by TEM (Fig. 5). Apart from areas where no CNT is found, CNTs are packed in bundles and tightly entangled.

As a conclusion on the dispersion of fillers in the matrix, APP is rather homogeneously dispersed in epoxy, either alone or in combination with nanofillers. Furthermore, the size of APP particles corresponds to the specifications from the supplier, suggesting that the dispersion is good. Nanoparticles do not lead to similar conclusions. The incorporation of OMPOSS in the matrix, either alone or not, produces a material with POSS aggregates dispersed in the matrix. Visual observation of the material shows that there are aggregates. Finally, the dispersion of CNTs in epoxy containing APP is inhomogeneous. Big areas containing no CNTs are easily found and CNTs bundles lie in the whole material. Furthermore, small holes can be found in the matrix. They may result from the increased viscosity of the uncured resin once CNTs are incorporated in it. During the curing, gases cannot be easily evacuated and could create holes in the final material.

3.4. Thermal conductivity

The thermal conductivity of the different formulations between 20 and 200 °C has been evaluated (Fig. 6). Below T_g, the thermal conductivity of virgin epoxy increases along with the temperature. Once the T_g is reached, it stabilizes and then begins to decreases at 200 °C, probably because of the onset of the degradation of the polymer: breaking of network certainly decrease phonon mobility causing the decrease of the thermal conductivity. Epoxy_APP-5 has a constantly increasing thermal conductivity, but it slows down above T_g. The higher conductivity values recorded for this sample may be linked to the crystallinity of APP. Indeed, phonons are better transmitted in geometrically regular and strong bonds. As an example, heat conductivity is higher in crystalline regions of polymers than in amorphous ones [6]. Therefore, phonons can be accelerated in APP particles, which would explain the higher thermal conductivity observed for Epoxy_APP-5. It should be noticed that the thermal conductivity still increases after the T_g for Epoxy_APP-5 whereas there is a stagnation for Virgin epoxy.

The behaviour is not the same when APP and CNTs are combined. The thermal conductivity of Epoxy_APP-4.5_CNT-0.5 behaves closely to that of virgin epoxy. The thermal conductivity is almost constant below Tg, it is higher at 150 °C, but a decrease similar as virgin epoxy follows. The presence of CNTs hides the effect of APP. A recent publication reports the modification of the thermal conductivity by incorporation of CNTs in an epoxy matrix [7]. They observed a decrease of the thermal conductivity for a 1.6 vol.% content, and attributed it to the formation of CNTs bundles which limits phonon transfers at the interface between the matrix and CNTs. This is consistent with our observations. Concerning Epoxy_OMPOSS-5, the thermal conductivity increases constantly between 20 and 200 °C. It is close to Epoxy_APP-5 and Epoxy_APP-4.5_CNT-0.5 at 20 °C and has an intermediate behaviour at 200 °C. Finally, the thermal conductivity of Epoxy_APP-4_OMPOSS-1 slightly increases between 20 °C and 50 °C and is constant thereafter.

Fig. 7 shows the thermal diffusivity of the five epoxy formulations between 20 °C and 200 °C. It remains almost constant for virgin epoxy. The same measurements performed on a sample containing 0.5wt.% CNTs alone in the epoxy matrix shows a lower diffusivity, whatever the temperature [8]. In contrast, the thermal diffusivity of Epoxy_APP-5 is 2.5–3 times higher than that of virgin epoxy below the T_g, and almost twice as high above the T_g. The thermal diffusivity of Epoxy_APP-4.5_CNT-0.5 appears as a linear combination of the samples containing these fillers separately. However, the contribution of CNTs seems to hide that of APP. The thermal diffusivity of Epoxy_OMPOSS-5 remains almost constant up to 150 °C and increases at 200 °C. Finally, Epoxy_APP-4_OMPOSS-1 has an intermediate behaviour below the T_g, but the thermal diffusivity is closer to that of virgin epoxy at 200 °C.

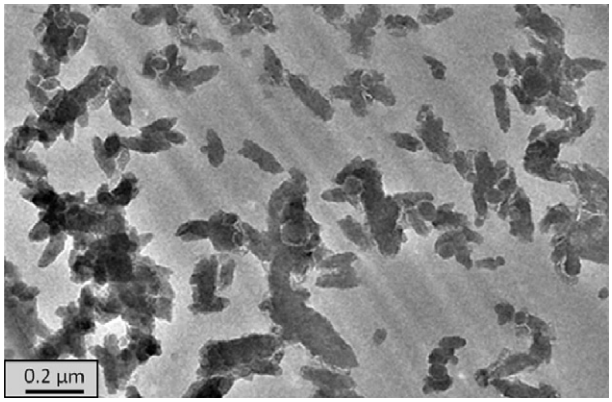


Fig. 4. TEM images of Epoxy_APP-4_OMPOSS-1.

3.5. Reaction to fire

In our previous article, we reported a synergy in terms of reaction to fire between APP and OMPOSS by mass-loss calorimetry. However, the high intumescence caused the blocking of the chimney of this apparatus. We propose here the same experiments, but with thinner samples (thickness = 2.5 mm instead of 5 mm in our previous article). The Heat Release Rate as well as the residual weight were recorded as a function of time. Fig. 8 and Table 3 show the fire-retardant performances of the different epoxy formulations. All formulations are characterized by a single peak of HRR. It

Please cite this article in press as: Gérard C, et al., Reaction to fire of an intumescent epoxy resin: Protection mechanisms and synergy, Polymer Degradation and Stability (2012), doi:10.1016/j.polymdegradstab.2012.05.025

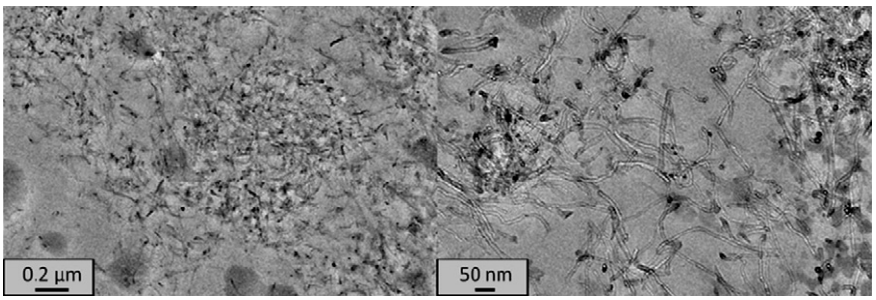


Fig. 5. TEM images of Epoxy_APP-4.5_CNT-0.5.

reaches 813 kW/m^2 for virgin epoxy. The incorporation of 5 wt.% OMPOSS in the matrix has a very limited effect since the pHRR is only decreased by 10%. Since this value lies within the error margins, OMPOSS does not have a significant fire retardant effect on the epoxy for thin samples.

Concerning intumescent systems, epoxy containing 5 wt.% APP exhibits a pHRR decreased by 31% compared to virgin epoxy. The reduced flame-retardant performance compared to that shown in thick samples (i.e. −50%) can be explained by the same phenomenon as above. In order to insulate the underlying polymer, the protective layer needs to be thick enough. Because of this, few polymer is protected in thin samples and the flame-retardant effects are not so strong. Combinations between APP and nanoparticles were also evaluated. Mixing CNTs and APP still leads to an antagonism (28% pHRR decrease), although it is limited compared to thick samples. In contrast, Epoxy_APP-4_OMPOSS-1 provides interesting properties since the pHRR is decreased by 50% compared to virgin epoxy, therefore showing the best results.

The time to ignition (TTI) is also influenced by the incorporation of flame retardants in the epoxy (Fig. 8 and Table 3). Virgin epoxy ignites after 49 s. TTI for samples containing APP or OMPOSS alone lies in the same range (46 and 50 s) respectively. In contrast, it is significantly reduced for the combinations between APP and nanoparticles. The presence of CNTs leads to the fastest ignition (37 s), followed by APP/OMPOSS (41 s).

The Total Heat Released (THR) is also reported in Table 3 for thin epoxy formulations. Thanks to lower amount of polymer with thin samples, no blocking of the extracting chimney occurred and the calculation of THR was therefore possible. The THR for virgin epoxy reaches 33 MJ/m^2. Confirming its limited interest for the flame retardancy of thin samples, incorporation of OMPOSS alone increases this value up to 36 MJ/m^2 (+9%). Intumescent systems lower it. Indeed, APP and APP/CNTs give similar results with 26 and 24 MJ/m^2 respectively (21 and 24% decrease) and APP/OMPOSS further decrease it by 30%.

Finally, the residual weight was recorded as a function of time (Fig. 9 and Table 3). All samples degrade in a single step. Before ignition (i.e. before 49 s), virgin epoxy keeps more than 95 wt.% of its initial weight. Then, burning leads to the very quick degradation of the resin, and between 50 s and 80 s, 87 wt.% of the sample are lost. The remaining and non-cohesive residue is then slowly degraded. The final residue amounts to 4 wt.%. The sample containing OMPOSS has a similar behaviour. 95 wt.% of the sample are intact before ignition, which occurs at 50 s. At 90 s, only 8 wt.% of the sample remains. Therefore, the main weight loss is extended to a slightly longer period, but the final residue is very similar (3 wt.%). This further shows the limited interest of OMPOSS alone as a flame-retardant for thin epoxy samples.

Intumescent systems begin to degrade earlier, but they do so as to stabilize the system at the end. The sample containing APP alone begins to lose weight before ignition: 90 wt.% of the specimen remain at 35 s, but the ignition occurs only at 46 s (ammonia is released during the degradation of APP and is not flammable). At this time, the sample keeps only 64 wt.% of its initial weight. Shortly after 50 s, the system stabilizes, the weight loss slows down and the final residue reaches 12 wt.%. The curve corresponding to APP/CNTs is very similar, except that the ignition (37 s) and the beginning of the degradation occur simultaneously.

From that point of view, this system behaves similarly to virgin epoxy or Epoxy_OMPOSS 5. However, the final residue is higher

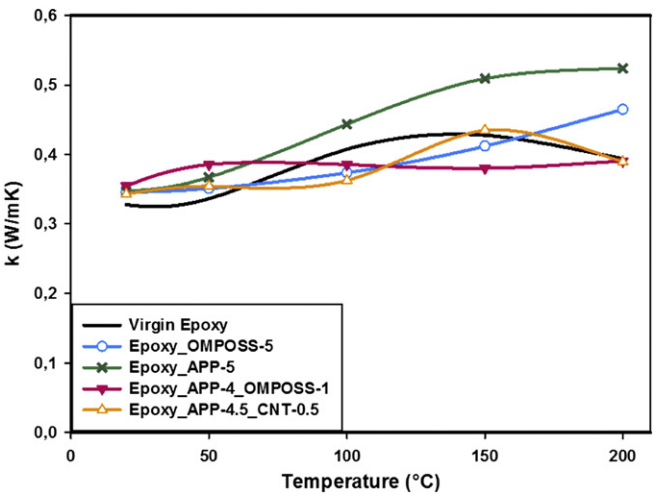


Fig. 6. Thermal conductivity of epoxy formulations.

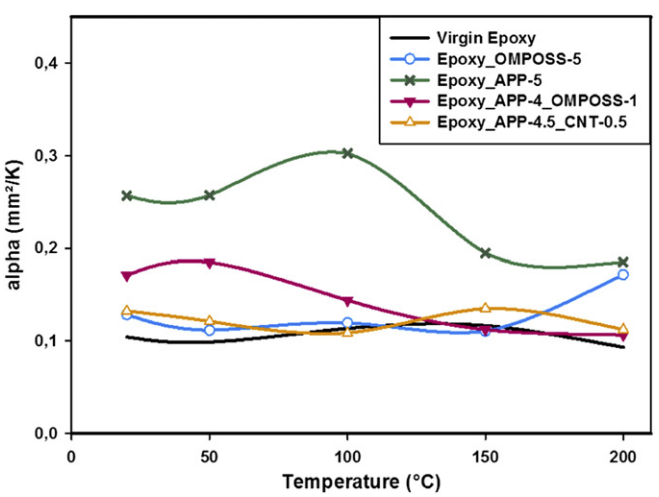


Fig. 7. Thermal diffusivity of epoxy formulations.

Please cite this article in press as: Gérard C, et al., Reaction to fire of an intumescent epoxy resin: Protection mechanisms and synergy, Polymer Degradation and Stability (2012), doi:10.1016/j.polymdegradstab.2012.05.025

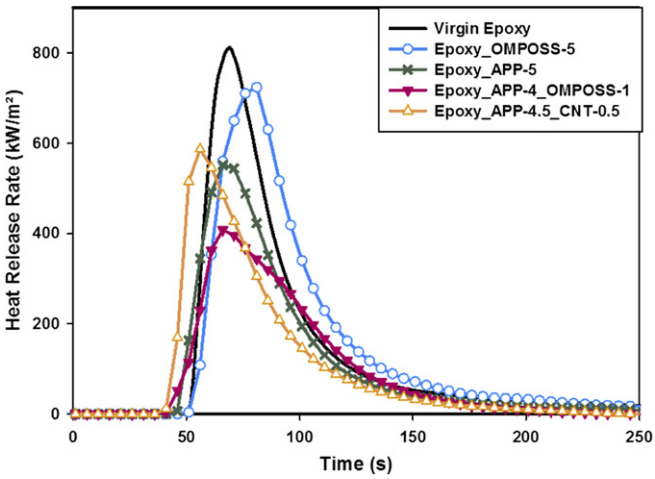


Fig. 8. Heat release rate as a function of time for epoxy formulations.

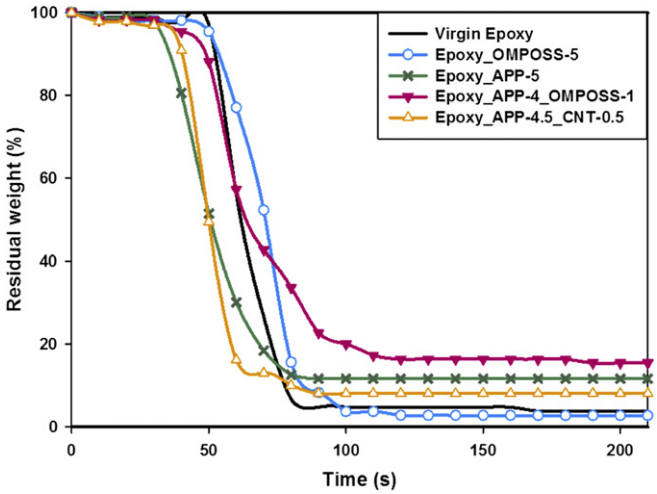


Fig. 9. Residual weight versus time for epoxy formulations.

(8 wt.%). This is another evidence of disturbances induced by CNTs in the intumescent system. Finally, the sample containing both APP and OMPOSS loses its weight later. It ignites at 41 s, when 95 wt.% of the sample remains. Then, the weight is lost very slowly: at 90 s, when the other samples lie between 5 and 12 wt.%, APP/OMPOSS still has 22 wt.% left. The final residue is also higher (15 wt.%). This fact further shows the interest of the incorporation of OMPOSS in Epoxy_APP 5.

As a first conclusion on the fire properties of the epoxy formulations, the use of OMPOSS alone is beneficial only for thick samples. This can be linked to the efficiency of the protective silica layer created on top of the specimen during burning. It has to be thick enough and in the case of thin samples, this can only be achieved when an important part of the polymer has already burnt. Intumescent systems give promising results. Combinations between APP and nanoparticles show how important the nature of the nanofiller is. CNTs lead to an antagonism, whereas OMPOSS provides a synergy.

3.6. Morphology of char during combustion

In this part, mass-loss calorimetry experiments were stopped at characteristic times of the HRR curve. The selected times are “just before ignition”, “at pHRR” and “at 500 s”, corresponding to the end of the experiment. For intumescent specimens, experiments were also stopped “during swelling”. First, the general aspect of these residues is described.

Samples removed from the heat source just before ignition are blackened but inhomogeneously deteriorated (Fig. 10). They will not be studied in the following. Pictures of the residues of Virgin epoxy at pHRR and 500 s are shown in Fig. 10. At pHRR, part of the epoxy is swollen into a black and cohesive residue. However, an important area of the material has been completely degraded, and the underlying aluminium foil is even destroyed. The residue after 500 s shows the foil only partially covered by a thin black powder.

Table 3
Mass-loss calorimeter main parameters for epoxy formulations.

Formulation	t_{ign} (s)	pHRR (kW/m^2) (% reduction)	THR (MJ/m^2) (% reduction	Residual weight (wt.%)
Virgin epoxy	49	813	33	4
Epoxy_OMPOSS-5	50	731 (−10)	36 (+9)	3
Epoxy_APP-5	46	557 (−31)	26 (−21)	12
Epoxy_APP-4.5_CNT-0.5	37	587 (−28)	25 (−24)	8
Epoxy_APP-4_OMPOSS-1	41	408 (−50)	23 (−30)	15

The morphology of Epoxy_OMPOSS-5 residue at pHRR and at 500 s is shown in Fig. 11. At pHRR, the residue is well-structured. The whole surface of the initial sample is covered by a black and smooth residue (Fig. 11a). Examination of the cross-section reveals that the inside consists of big cells Fig. 11b. The drawback of this residue is its excessive stiffness resulting in fragility. In fact, at 500 s, only a collapsed black and white material similar to ashes is recovered (Fig. 11c and d). Therefore, a protective structure is created during burning thanks to the presence of OMPOSS. However, it does not resist long enough. The white regions at the end of the experiment are ascribed to silica produced during combustion [9].

Stopping mass-loss calorimeter experiments at different times permits to observe the development of the intumescent structure in Epoxy_APP-5. Once the swelling has begun, the material begins to expand (Fig. 12). The whole surface of the initial sample is covered by a black crust (Fig. 12a). Large cells are created in the structure (Fig. 12b). However, it is noteworthy that these cells are empty and that the residue does not contain any foam at this point. Then, at pHRR, a vitreous residue is observed at the bottom of the sample (Fig. 12c). The initial material is therefore sufficiently preserved so that there is still epoxy at the bottom of the sample. Fig. 12d shows that the material is fully expanded into a very high structure with foam in it. Finally, at 500 s, the expanded char remains (Fig. 12e) but a brief look into the sample (Fig. 12f) reveals that there are big voids inside it.

Incorporation of CNTs in the Epoxy_APP-5 system induces important differences in the morphology of the residues along the testing. During swelling, there is an underlying polymer layer covered by a thin crust of carbonized material (Fig. 13a). However, this protective layer is very fragile and easily breakable. Fig. 13b shows that the residue obtained at pHRR covers the whole initial sample, but that small holes appear at its surface. Furthermore, the inner part of the sample is simply made of large cells (Fig. 13c) whereas there is an important foaming in epoxy containing APP alone. The morphology does not significantly change between pHRR and 500 s, as shown in Fig. 13d and e.

Epoxy_APP-4_OMPOSS-1 sample removed from the heat source during swelling is high compared to other formulations (Fig. 14a). Furthermore, a nice foamed structure is observed inside of the material (Fig. 14b), whereas Epoxy_APP-5 has only a hollow structure at the same time. Similarly to Epoxy_APP-5, the bottom of

Please cite this article in press as: Gérard C, et al., Reaction to fire of an intumescent epoxy resin: Protection mechanisms and synergy, Polymer Degradation and Stability (2012), doi:10.1016/j.polymdegradstab.2012.05.025

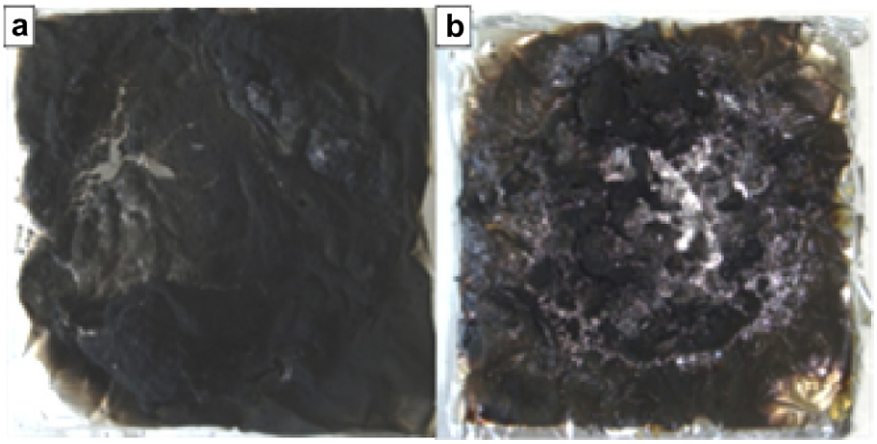


Fig. 10. Virgin epoxy residues during mass-loss calorimeter experiments (a: at pHRR, b: 500 s).

the sample at pHRR is black, solid and very dense, suggesting the presence of almost intact polymer at the bottom of the sample (Fig. 14c). A big char is created on top of it (Fig. 14d). Finally, at the end of the experiment, the structure is similar to the previous one (Fig. 14e and f). The char is well-structured with numerous voids inside. Interestingly, the upper part has a metallic appearance, whereas the lower one is black. This suggests that the material is not homogeneously deteriorated and that the upper part may protect the lower one.

3.7. Comparison between intumescent chars

The morphology of the chars after burning explains why a better behaviour is observed with Epoxy_APP-4_OMPOSS-1 than with Epoxy_APP-5. Fig. 15 shows vertical sections of the residues for Epoxy containing APP alone or combined with OMPOSS observed by digital microscopy. These pictures let us appreciate the extent of the foaming inside the samples. Areas containing big bubbles (Fig. 15, red circles in web version) are next to areas where small bubbles are mostly found (Fig. 15, blue rectangles). When APP is incorporated into epoxy alone, foaming occurs. Large bubbles are distinguished in the whole samples. In contrast, the combination between APP and OMPOSS leads to two different morphologies. Big bubbles are still produced, but mostly in the lower part of the sample. A large area with thinner ones is located on top of the residue. An evaluation of the size of the bubbles in the red circles reveals that the mean diameter lies about 1 mm in both cases. The size of the big bubbles is therefore similar in the two formulations. In contrast, the percentage corresponding to the area with almost only thin bubbles compared to the whole sample is 25% for Epoxy_APP-5 and 70% for Epoxy_APP-4_OMPOSS-1. Therefore, when the matrix does not resist to the internal pressure (presence of gases), big bubbles are created in both cases. However, these bubbles are mostly located at the bottom of the sample in the case of Epoxy_APP-4_OMPOSS-1 whereas they are found everywhere in Epoxy_APP-5. Subsequently, the percentage of the whole surface corresponding to denser areas (thin bubbles, blue rectangles on Fig. 15), which are supposed to provide a better protection against heat, is lower in the case of Epoxy_APP-5. Finally, because of the excess brittleness of the residue for APP/CNTs, it was not possible to analyse it.

A deeper insight into these bubbles is given by Fig. 16. Bubbles are linked together and they create a kind of network in both cases. However, the walls are thin in the case of Epoxy_APP-5 whereas the incorporation of OMPOSS in this system seems to partly fill the cavities and thicken the walls. Furthermore, during the cutting of the sample, Epoxy_APP-5 is brittle, whereas Epoxy_APP-4_OMPOSS-1 is much more resistant. It seems therefore that OMPOSS reinforces the structure of the char (at least mechanically).

Taking into account the different morphology of the chars when OMPOSS is incorporated in the Epoxy_APP-5 system, it was decided to analyse the distribution of phosphorus in the residues (the

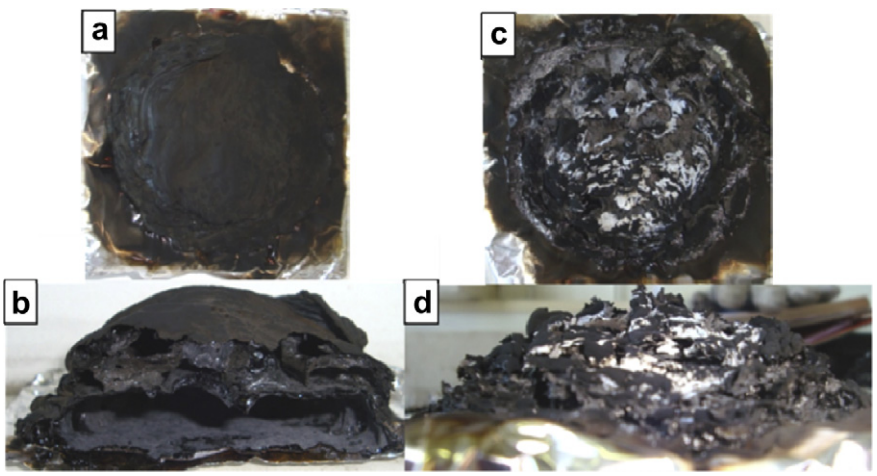


Fig. 11. Epoxy_OMPOSS-5 residues during mass-loss calorimeter experiments. At pHRR (a: top view, b: cross-section) and at 500 s (c: top view, d: cross-section).

Please cite this article in press as: Gérard C, et al., Reaction to fire of an intumescent epoxy resin: Protection mechanisms and synergy, Polymer Degradation and Stability (2012), doi:10.1016/j.polymdegradstab.2012.05.025

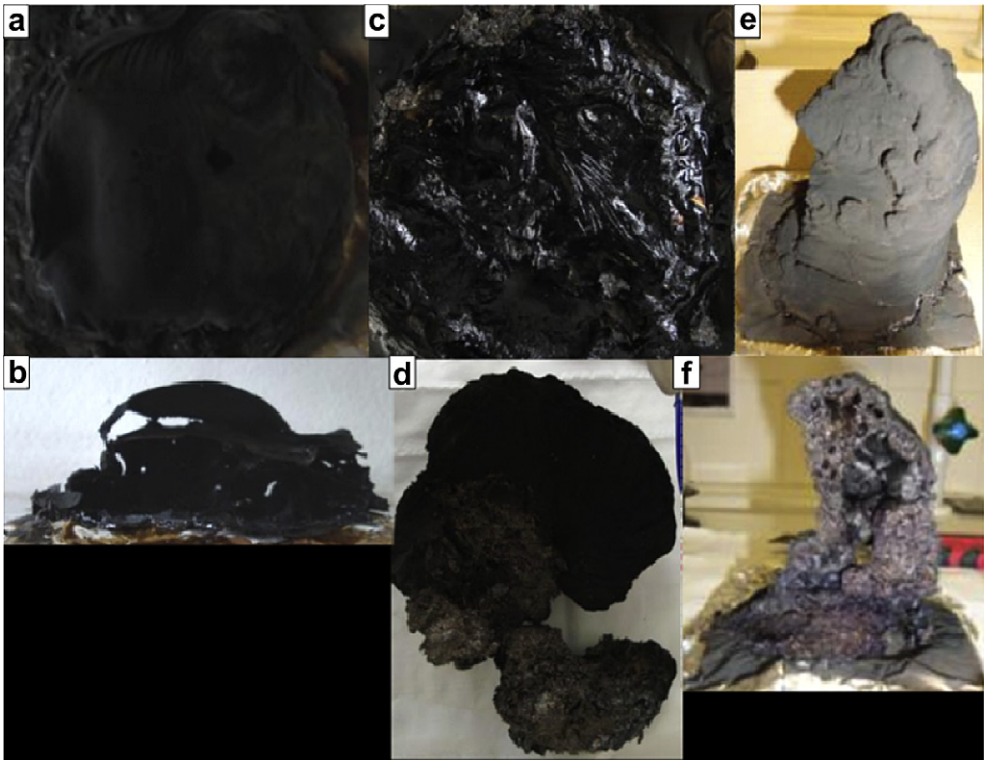


Fig. 12. Epoxy_APP-5 residues during mass-loss calorimeter experiments. During swelling (a: top view and b: cross-section), at pHRR (c: bottom of the residue and d: char), 500 s (e: top view and f: cross-section).

silicon concentrations were too low to be detected). The residues were studied by electron-probe microanalysis (EPMA) (Fig. 17). In order to get a better detection of phosphorus in the sample, the results were obtained on samples containing 10 wt.% filler instead of 5 wt.% in the normal case. For both Epoxy_APP-5 and Epoxy_APP-4_OMPOSS-1, high levels of phosphorus are mostly located at the bottom of the samples. Moreover, the comparison of both formulations on top or at the bottom of the samples suggests that in the presence of OMPOSS, phosphorus is more evenly distributed in the residues. This is consistent with digital microscopy observations, which have shown that Epoxy_APP-4_OMPOSS-1 contained more thin bubbles than Epoxy_APP-5, i.e. that matter is more evenly distributed in the residue in the case of Epoxy_APP-4_OMPOSS-1. Since phosphorus is located in the walls surrounding the bubbles, the presence of small bubbles contributes to its even distribution.

3.8. Solid-state Nuclear Magnetic Resonance (NMR)

Establishing the absence of gas-phase action is useful: intumescence is a well-known condensed-phase phenomenon but the developed systems are completely new. Therefore, in order to eliminate any doubt on the possibility of a gas-phase action, gases evolved during the thermal degradation of epoxy formulations were analysed by FTIR but no difference was observed between the formulations by this method (results not shown) [8]. In the following section, only condensed-phase phenomena will therefore be considered.

The residues described in the previous section have been analysed by solid-state NMR in order to check if the differences in the morphologies obtained over time for all formulations could result from the creation of different chemical species.

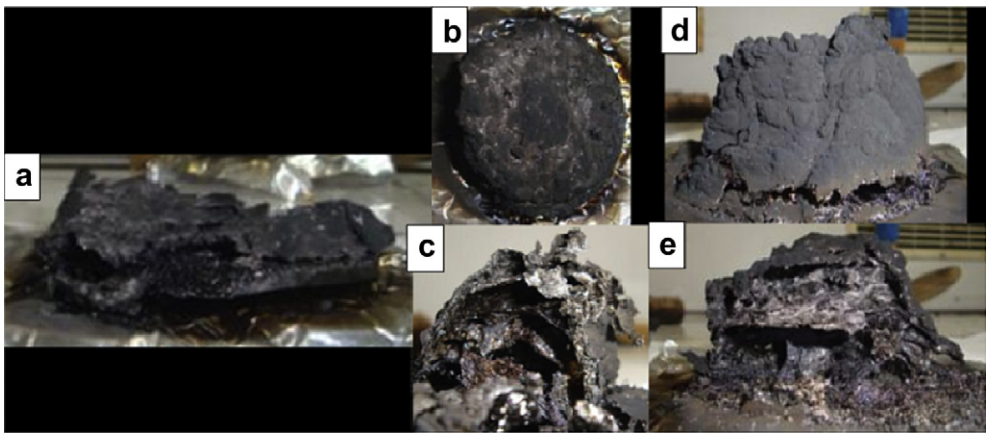


Fig. 13. Epoxy_APP-4.5_CNT-0.5 residues during mass-loss calorimeter experiments. During swelling (a: side view), at pHRR (b: top view and c: cross-section), 500 s (e: side view and f: cross-section).

Please cite this article in press as: Gérard C, et al., Reaction to fire of an intumescent epoxy resin: Protection mechanisms and synergy, Polymer Degradation and Stability (2012), doi:10.1016/j.polymdegradstab.2012.05.025

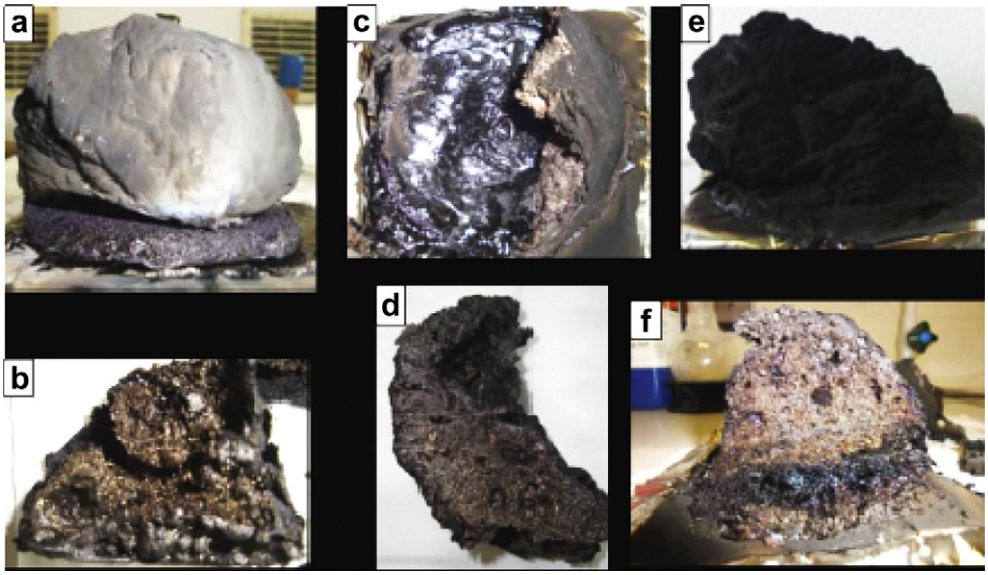


Fig. 14. Epoxy_APP-4_OMPOSS-1 residues during mass-loss calorimeter experiments. During swelling (a: side view and b: cross-section), at pHRR (b: top view and c: cross-section), 500 s (e: side view and f: cross-section).

3.9. Virgin epoxy

Even though the degradation of epoxy resins has been widely described in the literature [10], virgin epoxy residues have been analysed by solid-state NMR for later comparison with fire-retarded formulations. Fig. 18 shows the spectra of virgin epoxy residues at different times. The study of a non-degraded DGEBA cured with triethylenetetramine by Tavares et al. [11] has been used for assigning peaks of virgin DGEBA/DETA.

Nine wide peaks can be distinguished before degradation. The four peaks above 100 ppm correspond to the aromatic carbons of the DGEBA cycles. They are respectively assigned to C_4 (156 ppm, see Fig. 19), C_7 (143 ppm), C_6 (127 ppm) and C_5 (114 ppm). Carbons next to oxygen atoms in aliphatic ethers or alcohols give the peak at 69 ppm (C_3, C_{10} and C_{11}). The peak at 56 ppm comes from the C_{12}-N group resulting from the opening of epoxide ring during the curing of the resin. Unreacted epoxide rings can be identified at 41 ppm and 51 ppm (C_1 and C_2 respectively). The carbon linking the two aromatic rings also contributes to the peak at 41 ppm (C_8). Finally, the peak at 30 ppm comes from the CH_3 groups of the bisphenol A units (C_9).

The two other spectra correspond to further steps in the burning of the material: at pHRR and at 500 s. However, these spectra are very similar, showing that once the burning is initiated, the sample is very quickly deteriorated. A broad band is observed at 127 ppm. The broadness of the band shows that there are non-magnetically equivalent carbons. According to the literature, it is due to the carbonization of the material resulting in a condensed aromatic structure made of aromatic and polyaromatic species that are partially oxidized [12,13]. A band with low-resolution between 14 and 40 ppm is ascribed to the aliphatic degradation products of the resin. In fact, Rose et al. studied by ^{13}C solid-state NMR the degradation of an epoxy cured with diphenyldiaminosulfone [14]. They observed in particular a peak at 20 ppm attributed to methyl groups linked to aromatic species and another one at 14 ppm attributed to alkyl moieties, without further precision. This observation is consistent with the results for our resin. Then, once the material starts to burn, the degradation is very quick, as observed by the measurement of residual weight during mass-loss calorimetry. Epoxy polymer degrades, as evidenced by the NMR spectra showing the complete disappearance of the undegraded epoxy. The carbonization process takes place at pHRR.

3.10. Epoxy_OMPOSS-5

After the observation and characterization of the residues of the reference resin, the decomposition of the resin containing OMPOSS alone was studied. The residues of the non-intumescent OMPOSS formulation were analysed by ^{13}C and ^{29}Si solid-state NMR. ^{13}C NMR spectra are shown on Fig. 20. Before degradation, the spectrum exhibits almost the same peaks as virgin epoxy. An additional peak at −5 ppm is due to the methyl groups of OMPOSS. At pHRR,

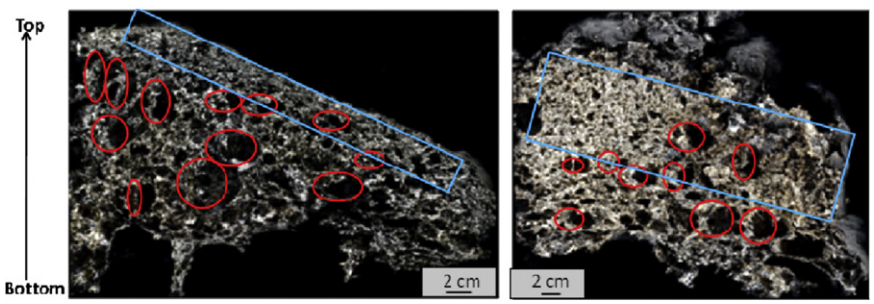


Fig. 15. Cross-sections of the whole residues from Epoxy_APP-5 (left) and Epoxy_APP-4_OMPOSS-1 (right).

Please cite this article in press as: Gérard C, et al., Reaction to fire of an intumescent epoxy resin: Protection mechanisms and synergy, Polymer Degradation and Stability (2012), doi:10.1016/j.polymdegradstab.2012.05.025

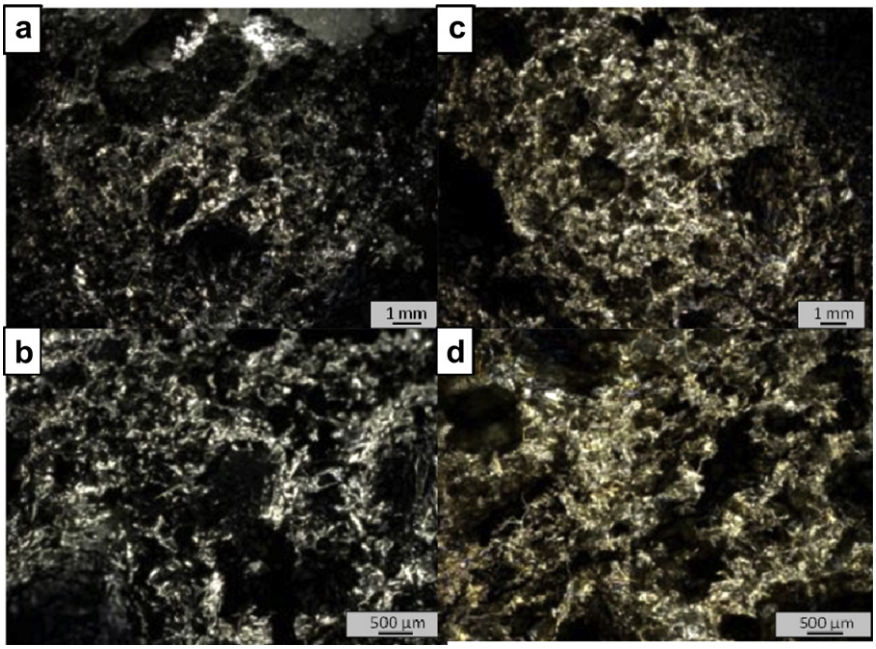


Fig. 16. Close-view of the bubbles in the char of Epoxy_APP-5 (left) and Epoxy_APP-4_OMPOSS-1 (right).

these peaks are still observed. Interestingly, OMPOSS and/or part of its degradation products remain in the structure (−5 ppm), although its specific band exhibits a lower resolution. Its peak enlargement is probably due to the loss of crystallinity when the sample is heated, as suggested by Vannier et al. [15]. Furthermore, this can also be ascribed to the breaking of some bonds in the POSS. Different structures coexist, but are still sufficiently close to each other for giving signals in the same chemical shift range [15]. In the aliphatic carbon range (10−30 ppm) bands are less defined due to the degradation of the polymer. Another important feature is the broadening of the peak at 127 ppm, which results in a unique band at the end of the combustion ($t = 500$ s). This is the only one band observed at 500 s, and is assigned to aromatic carbons constituting the char.

Therefore, the incorporation of OMPOSS in the resin does not change significantly the structure of the initial material. The interest of OMPOSS as flame-retardant is the preservation of epoxy resin at pHRR. It is not completely degraded and could explain the reduction of pHRR compared to the virgin epoxy. Since the carbonization process has begun, peaks are less defined, but the initial species are still present. However, this protection does not extend to the end of the experiment, since only carbons from the char are distinguished at 500 s.

The previous paragraph has shown that the epoxy resin was partially preserved until the pHRR is reached. The current one shows the ^{29}Si spectra and is aimed at identifying how long OMPOSS are present in the matrix (Fig. 21). Before commenting these results, the M, D, T and Q nomenclature on silicon species is

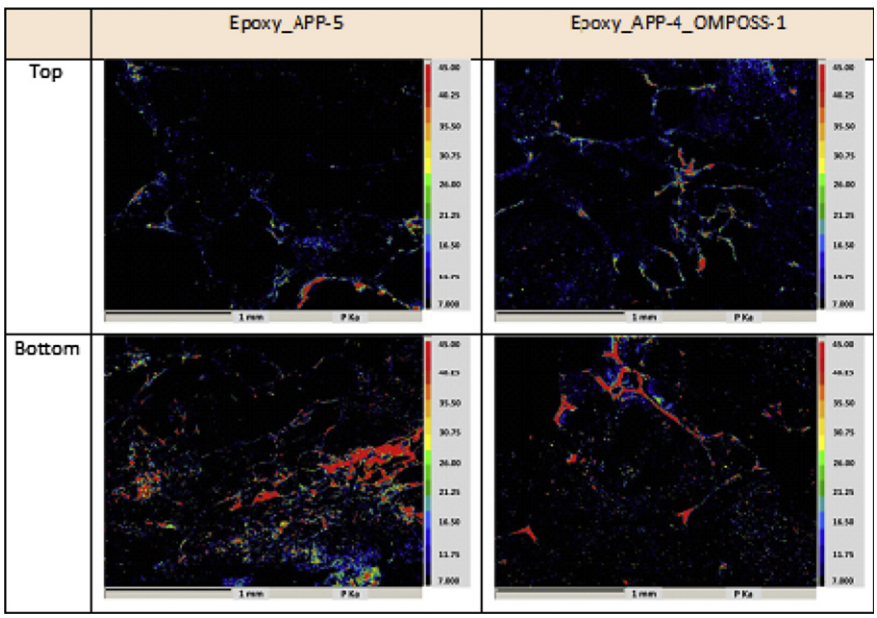


Fig. 17. EPMA mappings of phosphorus in the upper and lower parts of the char for Epoxy_APP-5 and Epoxy_APP-4_OMPOSS-1 (10 wt.% loading).

Please cite this article in press as: Gérard C, et al., Reaction to fire of an intumescent epoxy resin: Protection mechanisms and synergy, Polymer Degradation and Stability (2012), doi:10.1016/j.polymdegradstab.2012.05.025

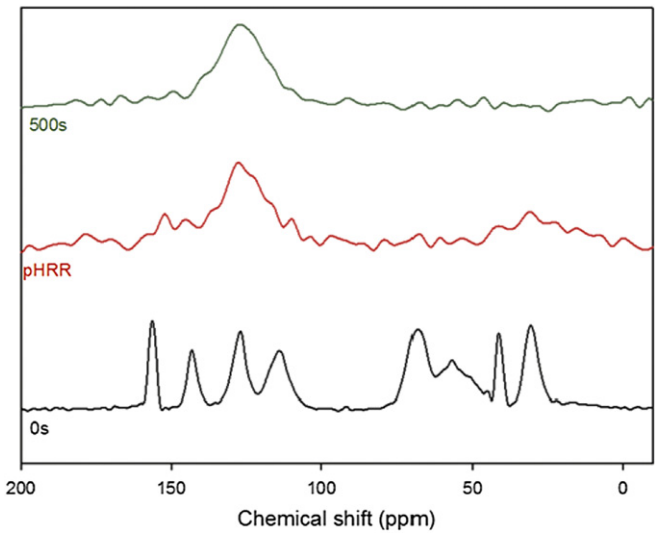


Fig. 18. ^{13}C CP-DD-MAS NMR spectra of the residues of Virgin epoxy at different mass-loss experiment times.

reminded on Fig. 22. This classification is based on the nature of the groups surrounding silicon atoms. Depending on the number of alkyl group linked to the silicon atoms, they will be referred to as M (3 alkyl groups), D (2 groups), T (1 group) or Q (no alkyl group). This classification is further specialized depending on the number of –O-Si- groups attached to the studied silicon atom. The nomenclature for T silicon atoms is described in Fig. 23: the *i* exponent is added to the previous classification to this end.

OMPOSS are characterized by a double peak at −66 ppm and −67 ppm in the non-degraded material (Fig. 21). Vannier et al. [15] have attributed them to silicon atoms T^3 linked to methyl groups on one side, and to three O-Si moieties on the other side. The presence of two peaks instead of a single one is probably due to the distortion of POSS cages in the powder, which results in different binding angles. At pHRR, these peaks are broadened and only a peak centred at −66 ppm is distinguished. Similarly to what has been observed for ^{13}C NMR, the breaking of POSS into smaller species associated to crystallinity loss is certainly the major cause of this phenomenon. At the end of the experiment, this peak is still observed, but an additional broad band lying between −100 and −120 ppm appears. According to Vannier et al. [15], the links between silicon atoms and methyl groups remain during the burning (−66 ppm). A larger silicon network is also created during the partial POSS decomposition, leading to the broad peak between −98 and −110 ppm attributed to silica [15].

Solid-state NMR reveals that the initial structure of the resin is preserved longer than for virgin epoxy, and that OMPOSS degrades in a mixture of broken cages and silica in the condensed phase.

3.11. Epoxy_APP-5

The degradation of intumescent systems has then been investigated. First, the reference intumescent epoxy, Epoxy_APP-5, has been studied. In this case both ^{13}C and ^{31}P NMR experiments were carried out on the residues. As shown by ^{13}C NMR (Fig. 24), the material before combustion is similar to virgin epoxy. During the swelling, two different layers have been identified. The bottom layer is made of almost intact resin, with peaks at 156, 143, 127, 114, 41 and 30 ppm. The upper one, In contrast, is already carbonized, as shown by the single peak at 127 ppm. The spectra corresponding to the same layers at pHRR are similar to the previous ones. The bottom layer shows characteristic peak of the epoxy resins. However, the peaks at 69 ppm (C-O) and 56 ppm (C-N) are broadened with low resolution and the band corresponding to CH_3 from the degradation products in the aliphatic carbon area is recorded. This indicates the decomposition of the resin, C-N and C-O bonds being one of the weakest points of the epoxy network [16]. The upper layer still shows only carbonized material. Finally, at 500 s, the bottom is also degraded and the spectra at the top and at the bottom are identical (only one of them is shown here). Once more, only aromatic carbons from the char are identified at 127 ppm.

Similarly to what has been done for Epoxy_OMPOSS 5, suitable nuclei were tracked in order to study how flame-retardants work. In this case, ^{31}P NMR spectra are shown in Fig. 25. Before degradation, APP exhibits a single band at −22 ppm (P-O-P links, here in polyphosphates). During the swelling, APP degrades (the spectra corresponding to the two different layers are similar and only one of them is shown). The peak at −11 ppm is attributed to the formation of orthophosphates linked to aromatic species and/or pyrophosphates [17]. The presence of phosphoric acid is revealed by the thin peak at 0 ppm. This is in accordance with the aforementioned mechanism of action of APP, which begins to degrade into ammonia and phosphoric acid. Furthermore, a well-defined peak at 30 ppm is attributed to phosphonic acid. Its presence will be discussed below. At pHRR, the vitreous bottom consists of three main bands centred at 0, −11 and −22 ppm. They are respectively attributed to phosphoric acid, orthophosphates linked to aromatic species and/or pyrophosphates, and P-O-P links of condensed phosphates [18]. An additional band is recorded at 16 ppm, and corresponds to phosphonate esters. These latter species, as well as phosphonic acid, are rather unexpected, since the initial flame-retardant is a phosphate. Their presence suggests therefore that a reductive phenomenon occurs during the burning. Karrasch et al. [19] have encountered a similar phenomenon while thermally treating a polycarbonate containing bisphenol A bis(diphenyl-phosphate). They attributed the formation of phosphonate esters to the graphitic structure of the char which could act as a possible reduction agent. In fact, the reduction of phosphates by graphite is used for the production of elemental phosphorus [20]. Even if no

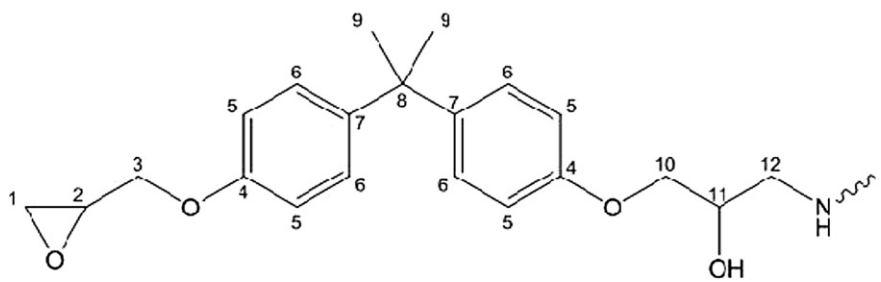


Fig. 19. Base structure of DGEBA/DETA epoxy resin.

Please cite this article in press as: Gérard C, et al., Reaction to fire of an intumescent epoxy resin: Protection mechanisms and synergy, Polymer Degradation and Stability (2012), doi:10.1016/j.polymdegradstab.2012.05.025

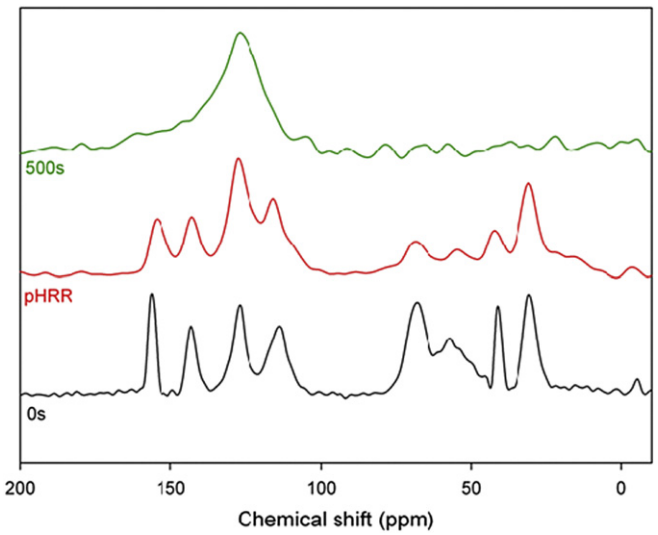


Fig. 20. ^{13}C CP-DD-MAS NMR spectra of the residues of Epoxy_OMPOSS-5 at different mass-loss experiment times.

other mention of such a phenomenon in the residues of polymeric materials was found, this explanation is reasonable: after ignition, reductive conditions are fulfilled near the flame. Furthermore, ^{13}C NMR has shown that carbonization has occurred on top of the sample, probably creating a pre-graphitic structure, as established by Raman spectroscopy by Bourbigot et al. [21].

The analysis of the char at pHRR shows similar peaks for the bottom and the top parts, with better defined ones on top. Phosphoric acid and orthophosphate linked to aromatic species or pyrophosphate are displayed by the peaks at 0 and −11 ppm. A large band centred at −23 ppm is recorded in the bottom spectrum and is attributed to condensed phosphates [13,22]. At the end of the experiment, peaks at 0, −11 and −23 ppm are present at the bottom of the sample and have the same attributions as before. On top of the sample, the only peak is that of phosphoric acid.

Therefore, the species produced during the burning of Epoxy_APP 5 and identified in ^{13}C and ^{31}P NMR are well-correlated with the mode of action of APP reported in the literature. An intumescent char is formed on top of residual material and protects it from a quick degradation.

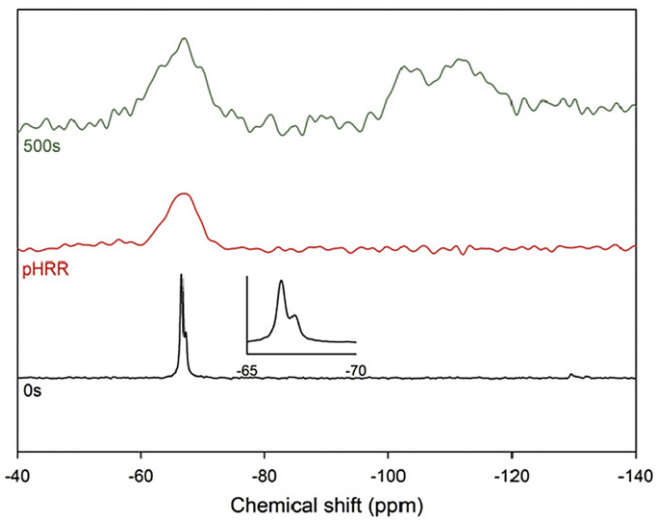


Fig. 21. ^{29}Si NMR spectra of the mass-loss calorimeter residues of Epoxy_OMPOSS-5.

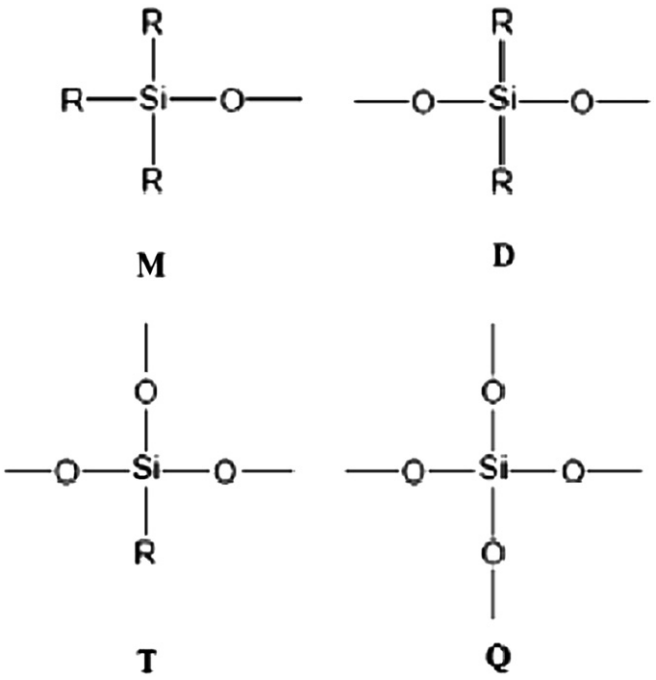


Fig. 22. M, D, T, Q nomenclature on silicon species.

After studying the degradation of Epoxy_APP-5 during mass-loss calorimetry experiment, the effect of the incorporation of nanoparticles in this system was assessed.

3.12. Epoxy_APP-4.5_CNT-0.5

Fig. 26 depicts the ^{13}C NMR spectra of the residues of Epoxy_APP-4.5_CNT-0.5. Before degradation, the spectrum is similar to that of virgin epoxy. During the swelling, the spectrum still shows the presence of residual polymer and also shows aliphatic product degradation. However, when pHRR is reached, there is only the characteristic peak at 127 ppm, showing that all carbons of the condensed phase contributed to the formation of the char. Therefore, contrarily to what happens with Epoxy_OMPOSS 5

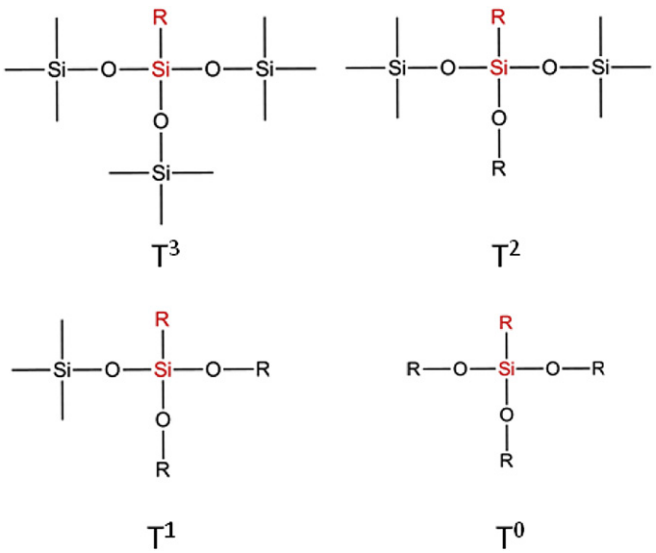


Fig. 23. T nomenclature for silicon atoms.

Please cite this article in press as: Gérard C, et al., Reaction to fire of an intumescent epoxy resin: Protection mechanisms and synergy, Polymer Degradation and Stability (2012), doi:10.1016/j.polymdegradstab.2012.05.025

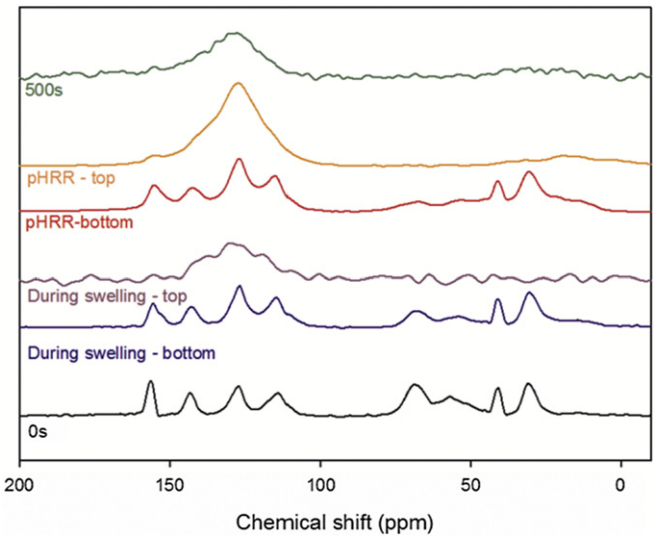


Fig. 24. ^{13}C CP-DD-MAS NMR spectra of the mass-loss calorimeter residues of Epoxy_APP-5.

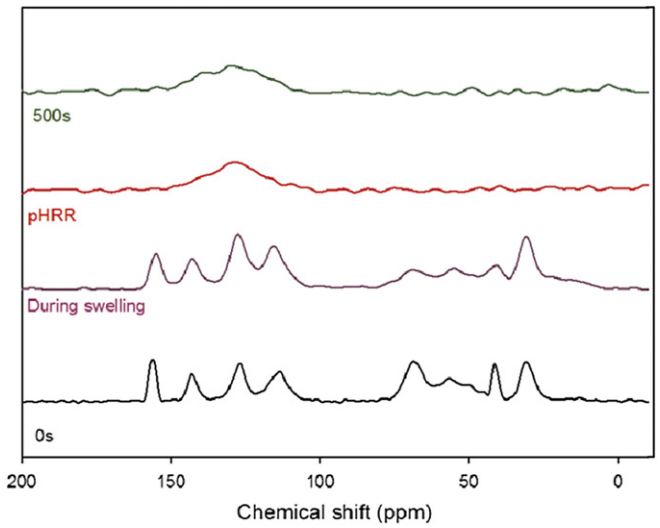


Fig. 26. ^{13}C CP-DD-MAS NMR spectra of the mass-loss calorimeter residues of Epoxy_APP-4.5_CNT-0.5.

or Epoxy_APP 5, there is no residual polymer in the material at pHRR. At 500 s, the peak at 127 ppm is the only one remaining.

Fig. 27 shows the ^{31}P NMR spectra obtained during the decomposition of Epoxy_APP 4.5_CNT 0.5. Before decomposition, the only peak (−22 ppm) is due to the presence of unreacted APP. During swelling, phosphoric acid (0 ppm) and pyrophosphates and/or orthophosphates linked to aromatic cycles (−11 ppm) are detected in the upper part of the sample. At its bottom, a broad band is observed between 0 and −22 ppm. Deconvolution of this broad band reveals it is made of three peaks corresponding to APP (−22 ppm), pyrophosphates and/or orthophosphates linked to aromatic cycles (−11 ppm) and orthophosphate linked to aliphatic carbons (−4 ppm). Therefore, APP is already well degraded on top of the polymer, whereas the decomposition has just begun inside the sample. At pHRR, two broad bands at 0 ppm and −11 ppm correspond respectively to phosphoric acid and pyrophosphates. A less visible one at −23 ppm is assigned to P-O-P links in condensed phosphates. At the end of the experiment, only phosphoric acid subsists.

The less effective morphology of the char created by Epoxy_APP-4.5_CNT-0.5, compared to Epoxy_APP-5, does not seem to come from additional created species. The only difference observed by solid-state NMR is that different layers can be identified in Epoxy_APP-5 whereas Epoxy_APP-4.5_CNT-0.5 is generally uniformly degraded. Furthermore, the peaks from the initial epoxy resin have completely disappeared at pHRR according to ^{13}C NMR spectrum of Epoxy_APP-4.5_CNT-0.5 while there is still residual polymer in Epoxy_APP-5.

3.13. Epoxy_APP-4_OMPOSS-1

The ^{13}C NMR spectra corresponding to Epoxy_APP-4_OMPOSS-1 (Fig. 28) are very similar to those of Epoxy_APP-5. Before degradation, peaks from the aromatic part of the resin are recorded at 156, 143, 127 and 114 ppm. Ether groups (CH-O and CH_2-O) have a contribution at 69 ppm. The chemical shifts of carbon linked to nitrogen atoms (CH_2-N and CH-N) appear at 56 and 50 ppm respectively. The peak at 41 ppm is due to unreacted epoxy rings.

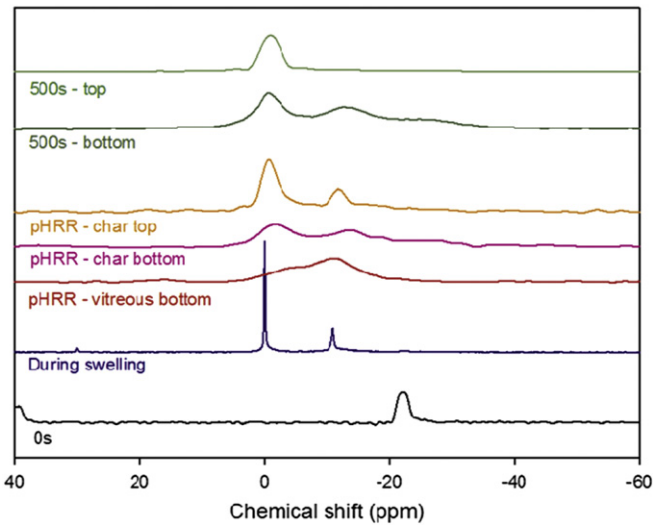


Fig. 25. ^{31}P NMR spectra of the mass-loss calorimeter residues of Epoxy_APP-5 (* = spinning sideband).

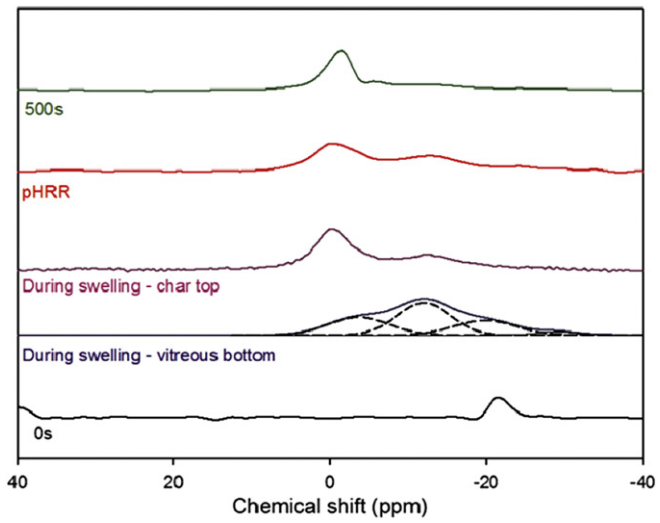


Fig. 27. ^{31}P NMR spectra of the mass-loss calorimeter residues of Epoxy_APP-4.5_CNT-0.5 (* = spinning sideband).

Please cite this article in press as: Gérard C, et al., Reaction to fire of an intumescent epoxy resin: Protection mechanisms and synergy, Polymer Degradation and Stability (2012), doi:10.1016/j.polymdegradstab.2012.05.025

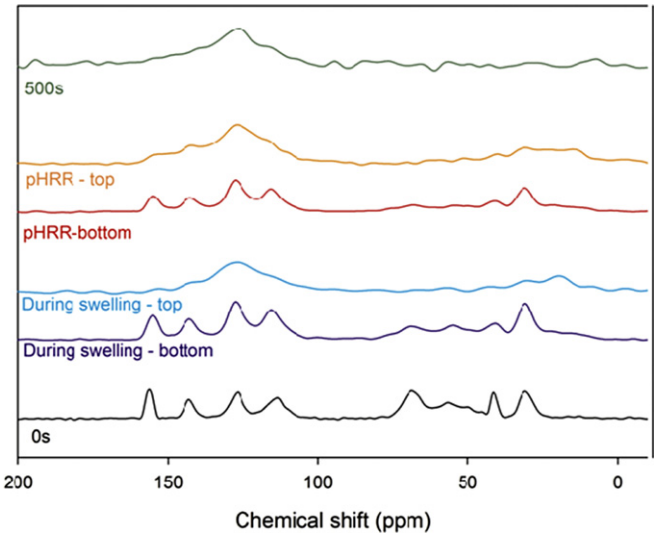


Fig. 28. ^{13}C CP-DD-MAS NMR spectra of the mass-loss calorimeter residues of Epoxy_APP-4_OMPOSS-1.

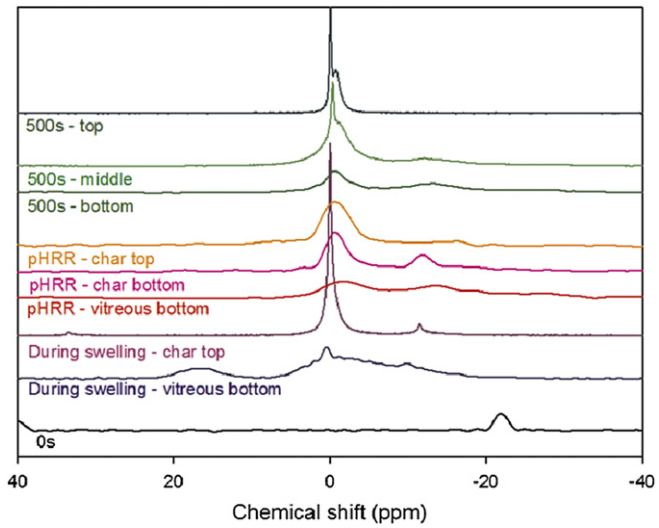


Fig. 29. ^{31}P NMR spectra of the mass-loss calorimeter residues of Epoxy_APP-4_OMPOSS-1 (* = spinning sideband).

Finally, CH_3 from the bisphenol-A unit are recorded at 30 ppm. The peak due to the methyl groups of OMPOSS is can also be distinguished at −5 ppm. During the swelling, whereas the same peaks are broadened at the bottom of the sample, aromatic carbons from the char appear on the upper part. The band due to aliphatic degradation products around 19 ppm appears and is still observed at pHRR. Furthermore, bands from the polymer at 155, 142, 127, 115, 69, 56, 41 and 30 ppm remain at the bottom of the sample when pHRR is reached. However, at the end of the experiment, only carbonized material remains.

The phosphorus-containing species encountered during the combustion of Epoxy_APP-4_OMPOSS-1 (Fig. 29) are close to that of Epoxy_APP-5. Before burning, unreacted APP leads to a peak at −22 ppm. During the swelling, analysis of the bottom reveals the presence of phosphoric acid (0 ppm), pyrophosphates and/or orthophosphates linked to aromatic cycles (−11 ppm) and phosphonate esters (17 ppm). On top of the sample, signals at 0 ppm and −11 ppm are assigned to phosphoric acid and pyrophosphates and/or orthophosphates linked to aromatic cycles. Phosphonic acid is detected at 33 ppm. The presence of reduced species can be explained by the same phenomenon as in Epoxy_APP-5 (graphitic species acting as reduction component). At pHRR, the vitreous bottom still contains phosphoric acid, pyrophosphates and/or orthophosphates linked to aromatic cycles and phosphonate esters. The bottom of the char contains the two first species and condensed phosphates (P-O-P, −22 ppm), whereas only phosphoric acid is identified in the top layer. Finally, at the end of the experiment, the bottom part contains phosphoric acid, pyrophosphate and/or orthophosphates linked to aromatic cycles and condensed phosphates. In the middle, phosphoric acid, orthophosphates linked to aliphatic carbons and pyrophosphates are observed. On top of the sample, only the two first species are identified. Therefore, in the case of Epoxy_APP-4_OMPOSS-1, no additional phosphorus-containing species is identified compared to Epoxy_APP-5.

The ^{29}Si spectrum before degradation shows only the thin peak of OMPOSS at −66 ppm (Fig. 30). During the swelling, the peak is broadened and is difficult to detect. On the other samples, no silicon peak could be detected. The best hypothesis about this phenomenon is that the combination between the low silicon content in the matrix and the impressive expansion of the sample dilutes the silicon too strongly. Therefore, the contents are so low that nothing can be detected. This also explains why the signal is already difficult to detect during the swelling. Because of this, it was decided to thermally degrade the mixture of APP and OMPOSS without matrix, in order increase the silicon content and try to detect any potential chemical reaction between the two fillers.

Thermogravimetric analyses under air were carried out on a mixture of APP and OMPOSS (ratio 4:1). The mixture degrades in two main steps at 250 °C and 620 °C (not shown) [8]. When comparing the experimental curve to the calculated one, the first step occurs at temperatures lower than calculated one (30 °C shift). It seems that the presence of APP might promote the degradation/sublimation of OMPOSS. There is no such modification for the last degradation step. However, the final residue is higher than expected (13 wt.% instead of 5 wt.%). It can be suggested that the APP residue partially traps and/or react with OMPOSS, therefore limiting the total weight loss. Indeed, this mixture was degraded under air in an oven and the residues were degraded. Analysing them by solid-state NMR does not reveal the presence of an additional species: depending on the temperature, mainly phosphoric acid,

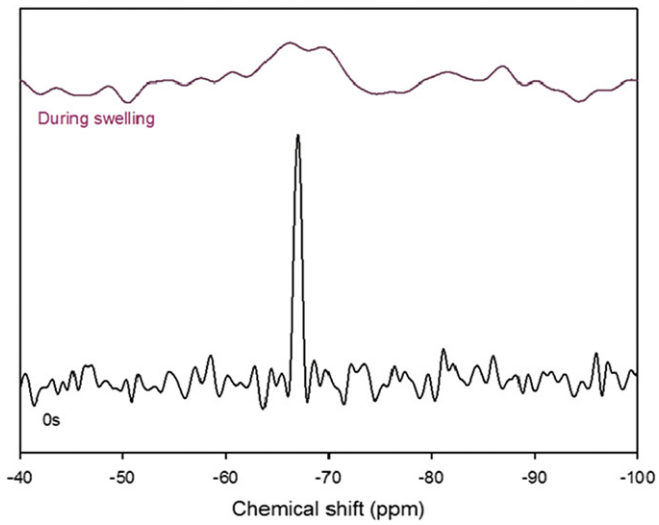


Fig. 30. ^{29}Si NMR spectra of the mass-loss calorimeter residues of Epoxy_APP-4_OMPOSS-1.

Please cite this article in press as: Gérard C, et al., Reaction to fire of an intumescent epoxy resin: Protection mechanisms and synergy, Polymer Degradation and Stability (2012), doi:10.1016/j.polymdegradstab.2012.05.025

pyrophosphates and P_4O_{10} are detected. However, the study of the same samples by X-ray diffraction suggests that silicophosphates (SiP_2O_7) are formed at high temperatures. The quantity is so low that if these silicophosphates are formed in the formulation, they reinforce only marginally the char of Epoxy_APP-4_OMPOSS-1.

Observations of the aspect of the residues over time for each formulation, combined to the analysis helps to understand the mechanisms involved in the reaction to fire of these formulations. Virgin epoxy degrades quickly into a non-cohesive char and no residual peak from the polymer can be seen by solid-state NMR. Incorporation of OMPOSS in it slows down the degradation of the polymer, since its peaks can still be detected at pHRR. The decomposition of OMPOSS produces a mixture of silica and degraded cages containing silicon. Furthermore, a structured residue is obtained at pHRR but it does not resist until the end of the test and collapses. APP alone in the epoxy resin degrades into ammonia, phosphoric acid and pyrophosphate. Links between the aromatic part of the resin and phosphorus-containing moieties can also be created, and reinforce the char. Indeed, an important intumescence occurs on top of this sample. The incorporation of CNTs in the Epoxy_APP-5 system does not modify the chemical species produced during its burning. However, the visual appearance of the residues suggests that the char does not develop so easily and it seems that a less effective protection is created. Then, Epoxy_APP-4_OMPOSS-1 also produces the same species as Epoxy_APP-5 upon thermal degradation. The difference between these two systems seems once more to lie in the structure of their char. During the swelling, a well-developed char exhibiting a foamed structure is observed with Epoxy_APP-4_OMPOSS-1, whereas the intumescent char is almost empty (large voids) with Epoxy_APP-5. Promotion of the degradation of OMPOSS by APP has been evidenced but no additional species explains this phenomenon. Therefore, it has been established that the antagonism and synergy phenomena do not lie in the creation of additional species. Because the observation of the residues suggests that physical parameters are modified, intumescence in dynamic conditions will then be studied in the following.

4. Viscosity

The previous paragraphs have established that no chemical reaction could explain the synergy observed in mass-loss calorimetry between APP and OMPOSS. The same comment can also be made for the sample containing both APP and CNTs, which displays an antagonistic behaviour. Furthermore, the observation of the residues at the end of the experiment and during it revealed that the structure of the char obtained is completely different. It has been shown by Jimenez et al. [23] that the efficiency of an intumescent system results from the right synchronization between the degradation of the resin and the release of gases. On the other hand, if the viscosity of the material is too low when gases are released, they cannot be trapped in the structure and the intumescence does not occur properly. In contrast, if the viscosity is too high, the materials cracks and gases are not correctly trapped either. Therefore, the next part is dedicated to the understanding of the formation of the char and the characterization of the protection provided. First, the viscosity of the different formulations will be recorded during thermal degradation. Then, the efficiency of the systems in terms of thermal protection will be assessed. The expansion of samples during mass-loss calorimetry experiments will also be evaluated. Finally, these parameters will be compared in order to propose a mechanism of action for these formulations.

The influence of nanofillers on the viscosity of epoxy resins has been widely discussed for processing issues [24]. Jimenez et al. [23] have shown that during the thermal degradation of an epoxy resin, a viscosity drop occurs. They have also observed that efficient flame-retardants limit this drop. Since the viscosity of the formulation is known for having an influence on the efficiency of intumescent systems [13], complex viscosity measurements were conducted between 25 °C and 500 °C on intumescent samples and virgin resin.

Fig. 31 shows the complex viscosity of virgin epoxy and intumescent formulations between 25 and 500 °C. Before the degradation of the materials, thermosets remain solid and the parallel plate viscosity measurements have no meaning. In contrast, when the materials degrade, they change into a viscous paste and viscosity data are available. TG curves have therefore been superposed to the viscosity measurements in order to detect relevant temperature ranges.

The viscosity is very similar for Epoxy_APP-5 and Epoxy_APP-4_OMPOSS-1 (5.6×10 [4] Pa s) and lower for Virgin epoxy and Epoxy_APP-4.5_CNT-0.5 (1.5×10 [4] Pa s) up to 320–350 °C. Then when the resin degrades, a viscosity drop is observed in all cases. The viscosity of Virgin epoxy decreases rapidly after 350 °C and it then increases quite rapidly after 370 °C, because of carbonization process. When APP alone is incorporated in the matrix, the viscosity decreases at lower temperatures (330 °C). Unfortunately, this formulation went over the edges of the sample holder during swelling and the final viscosity increase could not be properly recorded. However, it is noteworthy that the minimum viscosity lies in the same range as that of Virgin epoxy. The viscosity of Epoxy_APP-4.5_CNT-0.5 drops at 330 °C and its increases after 350 °C. The temperature range with a low viscosity is shifted

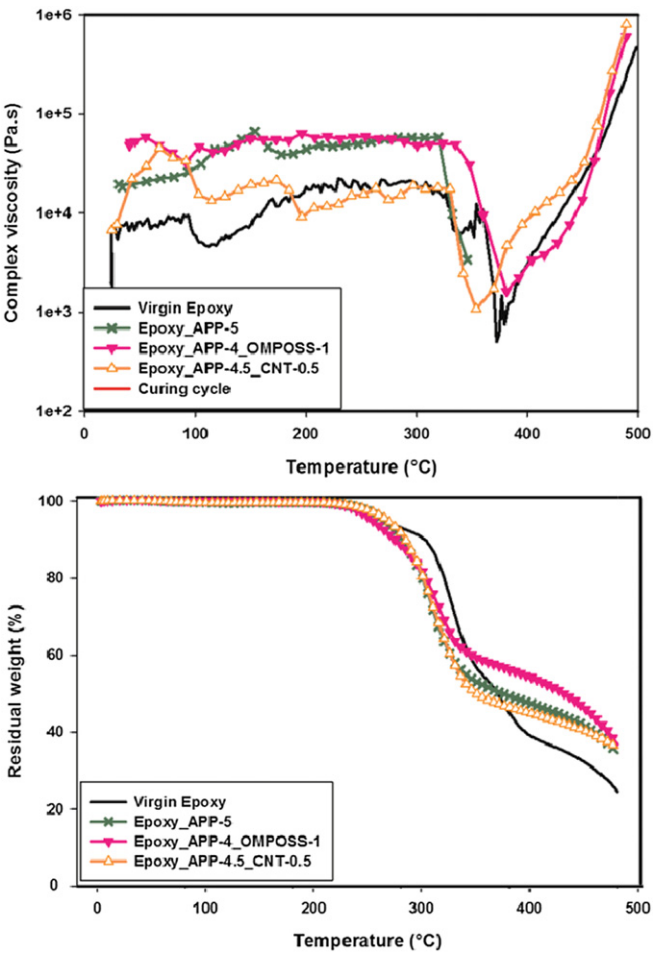


Fig. 31. Complex viscosity and TG curve of intumescent formulations as a function of temperature.

Please cite this article in press as: Gérard C, et al., Reaction to fire of an intumescent epoxy resin: Protection mechanisms and synergy, Polymer Degradation and Stability (2012), doi:10.1016/j.polymdegradstab.2012.05.025

towards lower temperatures compared to Virgin epoxy. The viscosity drop at lower temperatures for Epoxy_APP-5 and Epoxy_APP-4.5_CNT-0.5 compared to Virgin epoxy is due to the release of liquid phosphoric acid by APP during its thermal decomposition combined to the catalytic properties of this acid on the decomposition of the epoxy network, as observed by TGA. Finally, in the case of Epoxy_APP-4_OMPOSS-1, the viscosity drop is shifted towards higher temperatures compared to APP alone (340 °C instead of 330 °C) and the minimum viscosity is shifted towards higher temperatures, even higher than for Virgin epoxy (380 °C). Furthermore, the minimum viscosity of Epoxy_APP-4_OMPOSS-1 (1616 Pa s) is higher than that of Virgin epoxy (500 Pa s) and Epoxy_APP-4.5_CNT-0.5 (825 Pa s). TG curves show that the degradation of Epoxy_APP-4_OMPOSS-1 begins at temperatures similar to other intumescent systems but that it is stabilized thereafter (higher transient residue and maximum degradation rate temperature). This is consistent with the viscosity drop observed at higher temperatures and with a higher viscosity. Therefore it seems that the presence of OMPOSS in the Epoxy_APP-5 system brings 'additional glue' to the system and so limits and delays the viscosity drop.

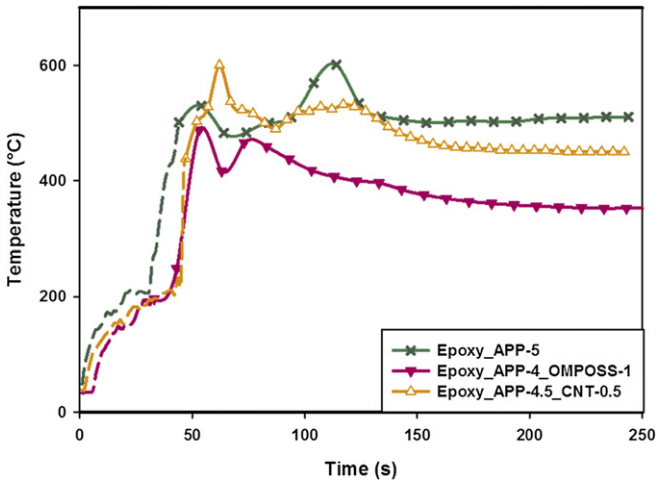


Fig. 32. Top temperature as a function of time during mass-loss calorimetry on intumescent samples (Heat flux: 35 kW/m^2, thickness = 25 mm, distance = 35 mm, T_{ign} = time to ignition). Dotted lines are used when thermocouples are not in the material.

5. Temperature gradient in intumescent char

In order to ensure that the performances of the flame-retarded samples were similar when thermocouple and infrared camera were used, the reaction to fire of the materials was assessed at a longer distance from the cone heater than in the standard conditions. First, an important fact is that TTI values are less reliable than when the samples are closer to the cone heater. Heat transfer via convection and radiation is then modified and the heating of the sample is changed. Furthermore, fumes are partially lost outside the chimney. All of this modifies the explosion diagram of the system, and since these modifications are partially erratic, TTI is less reliable. For all these reasons, the times to ignition will not be compared in this section, but only be used for knowing when the sample is starting to burn. The tendency between the efficiency of thin formulations shown before is not modified at this higher distance from the cone compared to standard conditions: the reductions of HRR are different but the formulation ranking is kept.

The major conclusions concerning the efficiency of the thin flame-retarded formulations are not modified when the distance from the cone is higher than in standard conditions. Therefore, in these conditions, the mass-loss calorimeter can be instrumented in order to get a better knowledge of the behaviour of our epoxy formulations.

Three thermocouples are inserted in the sample. One of them is located 1 cm above the sample and it will be embedded in the char for intumescent samples after swelling. The second one is inserted at the top surface of the sample, whereas the third one lies at the bottom of the sample. For each location, the results of the different formulations are compared.

The experiments with the thermocouple located 1 cm above were only carried out with intumescent formulations (Fig. 32). Before ignition, the samples show a similar temperature rate. The ignition results in a quick and large temperature increase. The temperature of Epoxy_APP-5 slightly increases after the ignition, up to 600 °C, then it cools down and the final temperature reaches 510 °C. Epoxy_APP-4.5-0.5 behaves very similarly and the final temperature is 450 °C, in the error margins of the experiment. Finally, the combination between APP and POSS leads to a much lower final temperature: 351 °C.

The maximum temperatures reached during the experiment give also interesting information. Epoxy_APP-5 reaches 601 °C at its maximum, whereas Epoxy_APP-4.5_CNT-0.5 goes up to 636 °C. This is in good accordance with mass-loss calorimeter results where these two formulations have similar performances. Furthermore, Epoxy_APP-4_OMPOSS-1 only reaches 502 °C during the experiment and provides better fire performances. Finally, it is noteworthy that only the thermocouple for Epoxy_APP-4_OMPOSS-1 is already in the matter when ignition occurs (i.e., the swelling is already important before ignition for this formulation).

For all formulations, the same analysis was conducted for the thermocouples on the surface of the samples (Fig. 33). Therefore, thermocouples are in the material from the very beginning of the sample. The trends are very similar between all samples except for virgin epoxy. At the end of the experiment, the highest temperature is measured for virgin epoxy (473 °C) but there is no residue left on it since the sample is almost completely destroyed, whereas it is lower for Epoxy/POSS (385 °C). Intumescent Epoxy_APP-5 reaches 416 °C at the end. The temperatures are lower for Epoxy_APP-4.5_CNT-0.5 and Epoxy_APP-4_OMPOSS-1 (351 °C and 289 °C respectively). An interesting feature is the maximum temperature reached. Virgin epoxy goes up to 766 °C, probably because the material is destroyed (and burns with high flames) and the thermocouple is in the fire. The samples containing POSS alone, APP alone and the combination between APP and CNTs reach similar temperatures (424 °C, 431 °C and 433 °C respectively). Epoxy_APP-4_OMPOSS-1 still remains in a lower temperature range (375 °C). Interestingly, the temperature for this last formulation decreases immediately and continuously after reaching its highest temperature, whereas a kind of plateau is observed for other formulations.

Finally, temperatures at the bottom of the samples were recorded (Fig. 34). Temperatures at the end of the experiment for epoxy containing OMPOSS, APP and APP/CNTs are close and reach respectively 310 °C, 305 °C and 282 °C. For Virgin epoxy, it is higher (428 °C), since there is almost no residue. In contrast, Epoxy_APP 4_OMPOSS 1 leads to lower temperatures (264 °C).

Differences are more important when looking at the maximum temperatures recorded. The temperature of Virgin epoxy always increases during the whole experiment and the final temperature is also the highest one (428 °C). This is consistent with the almost complete degradation of the sample (only ashes at the end). The temperature rate during the main increase is abrupt for Virgin epoxy (23 °C/s between 65 s and 74 s). This temperature rate is much lower for Epoxy_APP-4_OMPOSS-1, Epoxy_OMPOSS-5 and Epoxy_APP-4.5_CNT-0.5 (respectively 6 °C/s between 45 s and 75 s,

Please cite this article in press as: Gérard C, et al., Reaction to fire of an intumescent epoxy resin: Protection mechanisms and synergy, Polymer Degradation and Stability (2012), doi:10.1016/j.polymdegradstab.2012.05.025

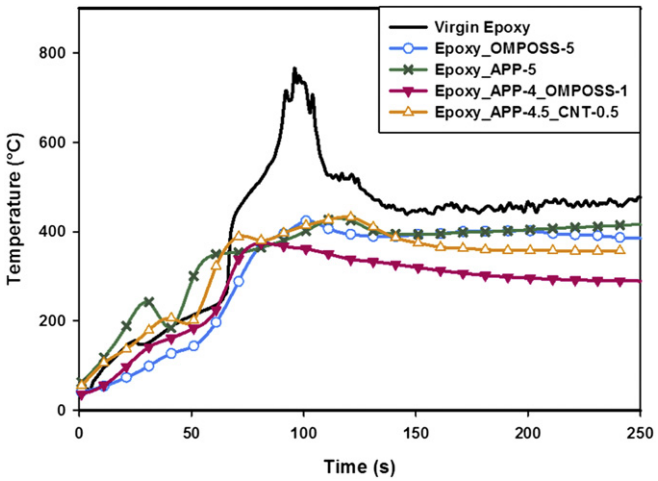


Fig. 33. Middle temperature as a function of time during mass-loss calorimetry on thin intumescent samples (Heat flux: 35 kW/m^2, thickness = 25 mm, distance = 35 mm, T_{ign} = time to ignition).

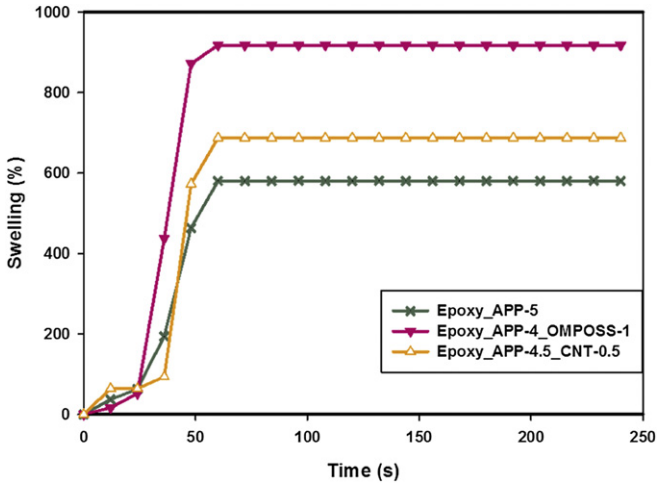


Fig. 35. Swelling as a function of time for thin intumescent systems (Heat flux: 35 kW/m^2, thickness: 25 mm, distance: 35 mm).

7 °C/s between 63 s and 80 s and 7 °C/s between 49 s and 72 s). It is even more reduced for Epoxy_APP-5 (2 °C/s between 41 s and 120 s). The maximum temperature reached by Epoxy_OMPOSS-5 is 322 °C, only 12 °C more than the final temperature for this formulation. For Epoxy_APP-5 and Epoxy_APP-4.5_CNT-0.5, the sample slightly cools down after the maximum temperature is reached (differences of 16 °C and 13 °C respectively). This difference is higher for Epoxy_APP-4_OMPOSS-1: 35 °C. However, this sample has the second highest maximum temperature after virgin epoxy. This apparent drawback could be the cause of the early protection formation observed previously (early degradation causing the formation of the protective structure more quickly).

6. Swelling of intumescent char

Fig. 35 shows the swelling of intumescent systems as a function of time. At the beginning, a first increase is recorded for all samples and remains below 100%. This phenomenon is likely due to the distortion of the sample (shrinkage) under the heat flux and cannot really be considered as a real expansion of the sample. This first artefact is then followed by the major development of the intumescent structure in a single step. This major increase begins at the same time for Epoxy_APP-5 and Epoxy_APP-4_OMPOSS-1 but the increase rate is higher in the presence of OMPOSS (40%/s for Epoxy_APP-4_OMPOSS-1 instead of 17%/s for Epoxy_APP-5). Taking into account that these POSS are known for subliming when heated [9], they should promote the quick development of the intumescent structure. In contrast, the sample containing CNTs begins to swell later, with a still high swelling rate (48%/s). However, it should be kept in mind that this high rate often ends with the cracking of the Epoxy_APP-4.5_CNT-0.5 residue. Concerning the swelling extent, APP alone leads to the lowest expansion (580%), quickly followed by Epoxy_APP-4.5_CNT-0.5 (687%). Epoxy_APP-4_OMPOSS-1 has the highest expansion with 918%. However, the final expansions are very similar for Epoxy_APP-5 and Epoxy_APP-4.5_CNT-0.5. Indeed, the samples are thin at the beginning (2.5 mm) and the char surface is not regular at the end: the difference between Epoxy_APP-5 and Epoxy_APP-4.5_CNT-0.5 is therefore only 3 mm and the final height can be considered as similar between these two formulations. These results on the swelling show that the development of the protection is affected by the presence of nanoparticles. OMPOSS enhances it, whereas CNT is a hindrance.

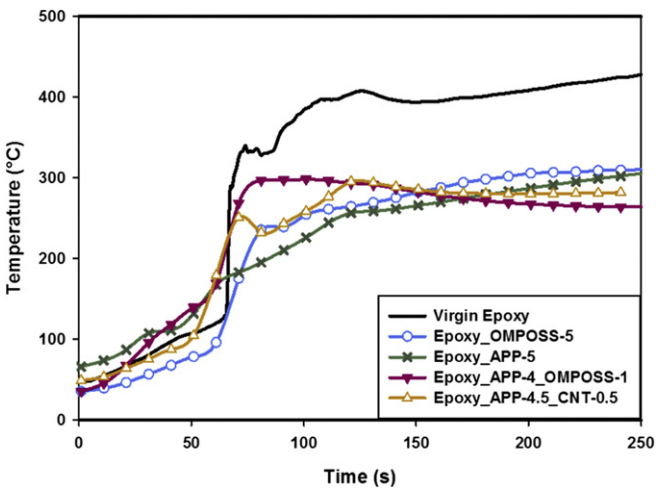


Fig. 34. Bottom temperature as a function of time during mass-loss calorimetry on thin intumescent samples (Heat flux: 35 kW/m^2, thickness = 25 mm, distance = 35 mm, T_{ign} = time to ignition).

Fig. 36 links the swelling to the weight lost during the burning. Indeed, if gases are not trapped during thermal decomposition, they may contribute to the development of fire (production of evolving flammable gases). If their trapping occurs, this should result in the swelling of the residue. Therefore, if the expansion is high with a low weight loss, gases are efficiently trapped in the samples. Furthermore, it means that the intumescent protection is created before most of the sample has degraded and the trapped gases contribute to the foaming (more foam in the char is supposed to enhance the thermal insulation).

The combination between APP and OMPOSS seems to have the most efficient swelling. Only 21 wt.% loss leads to a 687% swelling (Fig. 36). For the same weight loss, Epoxy_APP-5 exhibits an expansion of 273%, while Epoxy_APP-4.5-CNT-0.5 exhibits only 97% expansion. The maximum swelling is reached at 40 wt%, 59 wt.% and 48wt.% weight losses for the samples containing APP/OMPOSS, APP and APP/CNT respectively. This result evidences the ability of trapping degrading gases by the intumescent char developed by Epoxy_APP-4_OMPOSS-1. It is also noteworthy that the final residues are very similar for Epoxy_APP-5 and Epoxy_APP-4_OMPOSS-1. Indeed, there is not more material remaining at the end of the

Please cite this article in press as: Gérard C, et al., Reaction to fire of an intumescent epoxy resin: Protection mechanisms and synergy, Polymer Degradation and Stability (2012), doi:10.1016/j.polymdegradstab.2012.05.025

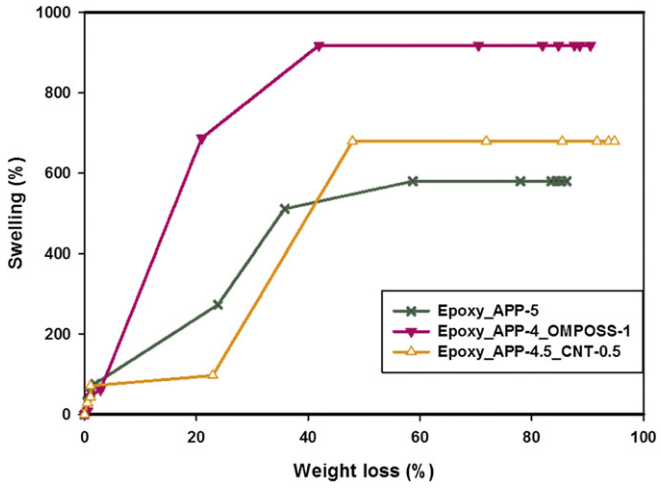


Fig. 36. Swelling as a function of weight loss for thin intumescent systems (Heat flux: 35 kW/m^2, thickness: 25 mm, distance: 35 mm).

experiment with OMPOSS than without, but the presence of OMPOSS delays the degradation and the instant release of fuels is lower. Subsequently, the flames are less energetic and the HRR is decreased. In contrast, when CNTs are incorporated, a higher weight loss is needed for developing the protection.

7. Swelling/temperature relationship

The previous experiments have revealed different phenomena. First, from the chemical point of view, no additional species is created when samples burn. Then, the physical characterization has shown that the structures of the residues created during the burning are different. Furthermore, it seems that intumescence occurs at slightly different times, which may explain why the temperatures reached inside the samples are lower for the most efficient formulations. The next figures propose to correlate these phenomena.

Fig. 37 shows the temperatures corresponding to the different thermocouples inside virgin epoxy, as well as the heat release rate. Briefly after ignition (determined with infrared camera), the two temperatures rise dramatically. The heat release rate begins to increase slightly later. In fact, epoxy often ignites with small flames on a limited area of the sample and the flames spread slowly on the whole sample. This may explain the shift between the ignition seen by infrared camera (direct observation of the flame at the surface of the sample) and on the HRR curve (measurement of fume temperature on top of the chimney). The middle temperature increases then steadily until pHRR is reached. After the first increase, the bottom temperature increases much slower up to the end of the experiment.

Similar observations were conducted on Epoxy_OMPOSS-5 (Fig. 38). An interesting feature is that the temperatures increase less quickly after ignition: the increase rate is 7 °C/s for Epoxy_OMPOSS-5 instead of 23 °C/s for Virgin epoxy. This suggests that the residue created by OMPOSS provides a better protection and that the system may also been cooled down by the endothermic sublimation of OMPOSS.

Epoxy_APP-5 is the first intumescent sample considered (Fig. 39). Contrary to previous samples, the ignition occurs simultaneously to the HRR increase, probably because of the intumescence, which set the surface of the sample closer to the spark igniter. At this time, all thermocouples are already in the material. The three temperatures rise in parallel and continue to slightly increase until the end of the experiment. It is noteworthy that intumescence begins before ignition and that the maximum expansion is reached just before the pHRR. An additional small peak is recorded for the top and the middle temperatures: it results probably from the partial cracking of the intumescent structure and the inflammation of released gases.

The presence of CNTs slightly modifies the previous behaviour (Fig. 40). The main difference is that HRR increases shortly after the ignition, and the temperatures make the same. An important fact is the expansion begins when the sample ignites and the maximum expansion is reached very quickly. It seems therefore that the structure created with APP and CNTs does not trap correctly the gases evolved during the combustion. This is consistent with the previous section linking the expansion and the weight loss: expansion is initiated with a higher weight loss in this sample. Taking into account the morphology of the different residues, the hollow structure of Epoxy_APP-4.5_CNT-0.5, combined with the presence of small holes on top of the specimen support this hypothesis.

Finally, the sample containing both APP and OMPOSS was studied (Fig. 41). Ignition occurs before the HRR increases, and the reached temperatures remain low. The main information is that the swelling occurs well before ignition and continues shortly

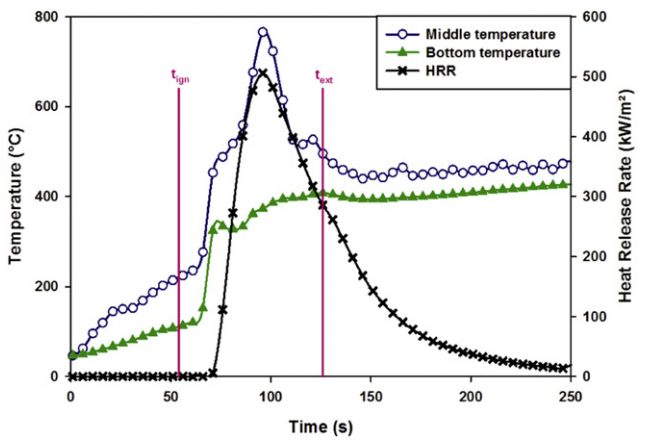


Fig. 37. Temperatures reached inside virgin epoxy and Heat Release Rate as a function of time (Heat flux: 35 kW/m^2, thickness: 25 mm, distance: 35 mm, t_{ign}: time to ignition, t_{ext}: time to extinction).

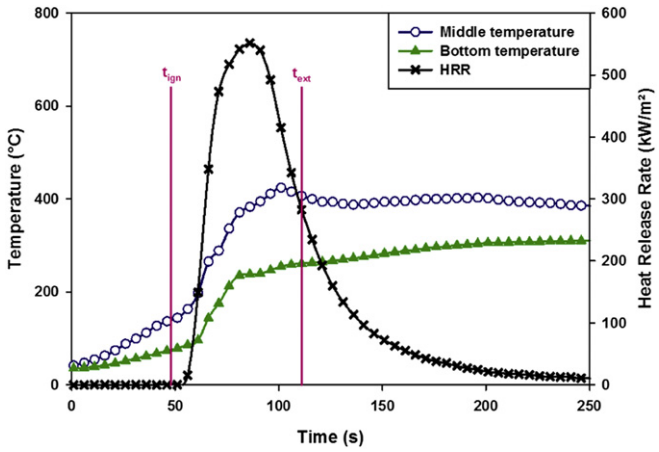


Fig. 38. Temperatures reached inside Epoxy_OMPOSS-5 and Heat Release Rate as a function of time (Heat flux: 35 kW/m^2, thickness: 25 mm, distance: 35 mm, t_{ign}: time to ignition, t_{ext}: time to extinction).

Please cite this article in press as: Gérard C, et al., Reaction to fire of an intumescent epoxy resin: Protection mechanisms and synergy, Polymer Degradation and Stability (2012), doi:10.1016/j.polymdegradstab.2012.05.025

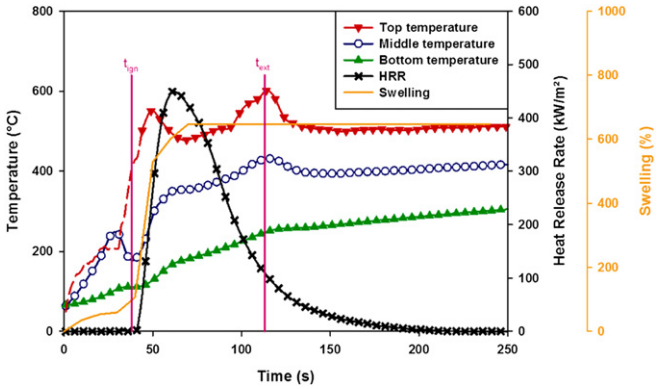


Fig. 39. Temperatures reached inside Epoxy_APP-5, Heat Release Rate and swelling as a function of time. (Heat flux: 35 kW/m^2, thickness: 25 mm, distance: 35 mm, t_{ign}: time to ignition, t_{ext}: time to extinction). The dotted line is used when the thermocouple is not in the material.

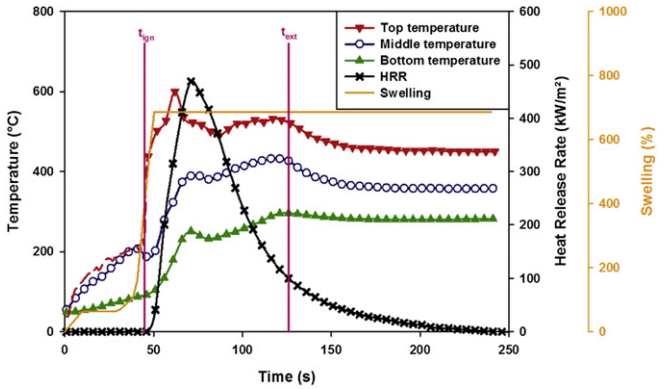


Fig. 41. Temperatures reached inside Epoxy_APP-4_OMPOSS-1, Heat Release Rate and swelling as a function of time. (Heat flux: 35 kW/m^2, thickness: 25 mm, distance: 35 mm, t_{ign}: time to ignition, t_{ext}: time to extinction). The dotted line is used when the thermocouple is not in the material.

thereafter. Comparing this to the behaviour of Epoxy_APP-5, it can be concluded that the early development of intumescence is useful but also that the intumescent structure has to be created before most of the sample is burnt. In the case of Epoxy_APP-5, the maximum expansion is reached too late. TGA experiments showed that OMPOSS sublimes shortly above 200 °C, whereas APP decomposes around 275 °C. Therefore, OMPOSS are trapped in the structure and contribute to the blowing of the structure. Indeed, between 200 and 300 °C, the resin has already begun to degrade and the shortened network should be able to trap these gases. The swelling is initiated when the top and middle thermocouples reach 200 °C. Another important fact is that the temperatures decrease just after pHRR is reached, whereas it went down long after for other intumescent formulations. A thicker structure is more easily created thanks to the presence of OMPOSS and it then better insulates the system.

8. General discussion and conclusion

The study of the species formed during the burning of Epoxy_OMPOSS-5 and Epoxy_APP-5 as well as the properties of the structure created have confirmed the mechanisms suggested in the literature. The thermal degradation of the sample containing OMPOSS is slowed, as shown by thermogravimetric analyses under air and nitrogen. The better behaviour of polymers containing POSS is generally attributed to the formation of silica as protective layer.

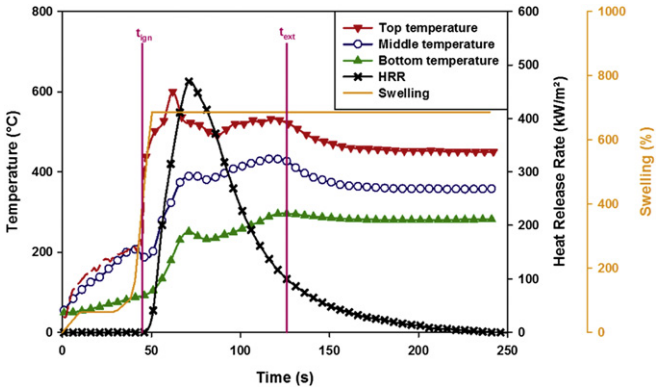


Fig. 40. Temperatures reached inside Epoxy_APP-4.5_CNT-0.5, Heat Release Rate and swelling as a function of time. (Heat flux: 35 kW/m^2, thickness: 25 mm, distance: 35 mm, t_{ign}: time to ignition, t_{ext}: time to extinction). The dotted line is used when the thermocouple is not in the material.

Wu et al. [25] have also suggested that a POSS bearing isobutyl moieties on part of its corners may act as a radical trap. The isobutyl radical would capture the hydrogen radicals formed during the combustion of the polymer and the silicon radical of the POSS would act similarly for hydroxyl radicals. A char with improved properties would be formed thereafter. This mechanism could be transposed to OMPOSS. However, without proof of the aforementioned mechanism, the main phenomenon occurring remains the formation of the silica layer, as observed on residues pictures. It should be pointed out that the fragility of the produced residue limits the enhancement of the reaction to fire.

The mechanism of action of APP is relatively well-known in thermoplastics but it is limited in thermosets. It degrades at temperatures lower than that of the polymer and releases ammonia in the gas phase while phosphoric acid is formed from its degradation and remains in the condensed phase. Phosphoric acid reacts with the degraded polymer to form a carbonaceous residue, whereas the release of ammonia makes it swell. The addition of CNTs to the Epoxy_APP-5 system modifies this otherwise well-organized mechanism. The species identified in the solid residue along the combustion do not differ from those observed in Epoxy_APP-5. CNTs do not therefore chemically interact with the other constituents. The swelling begins similarly as with APP alone, but it occurs very briefly. The thermal diffusivity is also significantly reduced compared to Epoxy_APP-5. These modifications may explain the antagonism between APP and CNTs. The development of the protective structure due to APP is not initially hindered by the presence of CNTs, but the char formed is not as resistant as before, and the continuous release of gases, which should expand it, gives cracks in the char. CNTs seem therefore to induce defects in the structure of the char resulting in its cracking and less efficient structure.

Finally, it has been shown that the intumescence occurs earlier with Epoxy_APP-4_OMPOSS-1, therefore offering a protection to the underlying material before further degradation. The development of this intumescent structure before ignition can be attributed to the combination between the release of ammonia by APP and the partial sublimation of OMPOSS. The lower temperatures reached by this formulation also give more time for the structure to foam, and to be subsequently better insulated. A char with improved mechanical resistance is produced. The better protection offered by this formulation is therefore due to the earlier formation of the char, which permits its better structuring.

All these mechanisms are summarized in Fig. 42. Epoxy_APP-5 begins to swell before ignition with a relatively low swelling rate.

Please cite this article in press as: Gérard C, et al., Reaction to fire of an intumescent epoxy resin: Protection mechanisms and synergy, Polymer Degradation and Stability (2012), doi:10.1016/j.polymdegradstab.2012.05.025

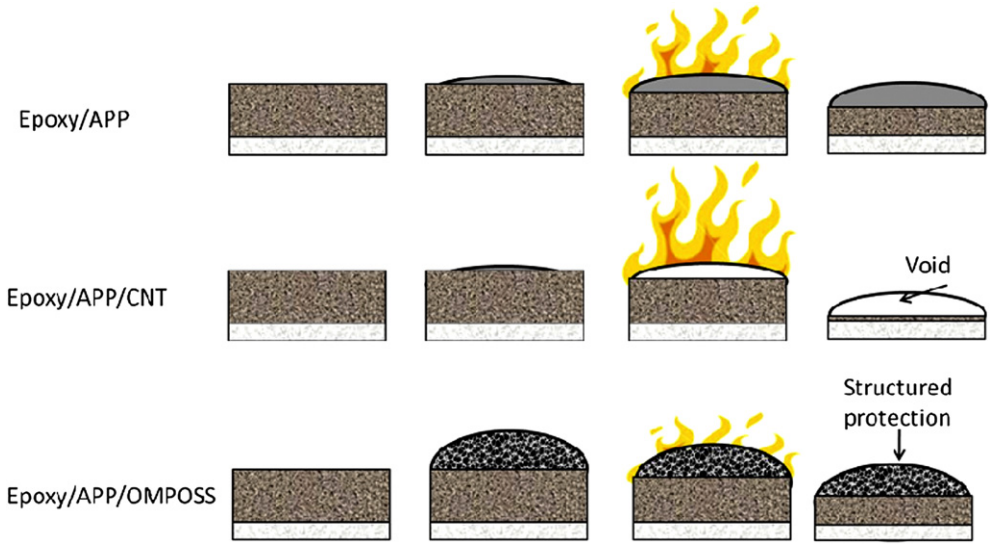


Fig. 42. Main protection mechanisms involved by the intumescent formulations.

Therefore, when ignition occurs and flames spread, the maximum expansion is not already reached. In the case of Epoxy_APP-4.5_CNT-0.5, the swelling is initiated relatively late. Furthermore, even if the protection develops with a high swelling rate, the structure does not resist to the internal pressure involved by the presence of gases and cracks appear. Finally, in the case of Epoxy_APP-4_OMPOSS-1, swelling occurs early and with a high swelling rate. Therefore, the maximum expansion is reached before fire spreads. Furthermore, the internal structure of the char provides better insulation.

In this study, the composition of the samples has been characterized at different times of the burning. OMPOSS alone in the epoxy matrix produces silica. The species identified in Epoxy_APP-4_OMPOSS-1 and Epoxy_APP-4.5_CNT-0.5 do not differ from those present in Epoxy_APP-5. The antagonism between APP and CNTs, and the synergy between APP and OMPOSS do not therefore originate in the creation of new species, even if phosphosilicates reinforcing the char may be produced in the case of Epoxy_APP-4_OMPOSS-1. Indeed, the dynamic study of the burning of the three intumescent samples reveals that the better behaviour of Epoxy_APP-4_OMPOSS-1 results mainly from an adequate viscosity that facilitates the trapping of degradation gases in the material and favours its structured expansion. In contrast, the excessive stiffness of the residue of Epoxy_APP-4.5_CNT-0.5 does not allow the correct development of the protective structure.

Acknowledgements

The research leading to these results has received funding from the European Community's Seventh Framework Programme (FP7/2007-2013) under the grant agreement no 213267 – LAYSA "Multifunctional Layers for Safer Aircraft Composites Structures".

References

[1] Lyon RE. In: Horrocks AR, Price D, editors. Advances in fire retardant materials. Woodhead Publishing; 2008.
[2] Gérard C, Fontaine G, Bourbigot S. Polymers for Advanced Technologies 2011; 22:1085–90.
[3] Zhang Z, Liang G, Ren P, Wang J. Polymer Composites 2008;29:77–83.
[4] Allaoui A, El Bounia N. Express Polymer Letters 2009;3:588–94.
[5] Samyn F, Bourbigot S, Jama C, Bellayer S. Polymer Degradation and Stability 2008;93:2019–24.
[6] Han Z, Fina A. Progress in Polymer Science (Oxford); 2011.
[7] Teng CC, Ma CCM, Chiou KC, Lee TM, Shih YF. Materials Chemistry and Physics, 126, 722–728.
[8] Gérard C, Ph.D thesis, University of Lille 1, 2011.
[9] Fina A, Tabuani D, Carniato F, Frache A, Boccaleri E, Camino G. Thermochimica Acta 2006;440:36–42.
[10] Levchik SV, Weil ED. Polymer International 2004;53:1901–29.
[11] Tavares MIB, D'Almeida JRM, Monteiro SN. Journal of Applied Polymer Science 2000;78:2358–62.
[12] Bourbigot S, Duquesne S. Journal of Materials Chemistry 2007;17:2283–300.
[13] Jimenez M, Duquesne S, Bourbigot S. Thermochimica Acta 2006;449:16–26.
[14] Rose N, Université des Sciences et Technologies de Lille, PhD thesis, 1995.
[15] Vannier A, Duquesne S, Bourbigot S, Alongi J, Camino G, Delobel R. Thermochimica Acta 2009;495:155–66.
[16] Grassie N, Guy MI, Tennent NH. Polymer Degradation and Stability 1986;14: 125–37.
[17] Assaaoudi H, Butler IS, Kozinski J, Bélanger-Gariépy F. Journal of Chemical Crystallography 2005;35:809–20.
[18] Bourbigot S, Le Bras M, Delobel R, Trémillon JM. Journal of the Chemical Society - Faraday Transactions 1996;92:3435–44.
[19] Karrasch A, Wawrzyn E, Schartel B, Jäger C. Polymer Degradation and Stability 2010;95:2525–33.
[20] Van Wazer JR. Phosphorus and its compounds, vol. 1:Chemistry, Interscience Publishers Inc.
[21] Bourbigot S, Bras ML, Delobel R. Carbon 1993;31:1219–30.
[22] Bugajny M, Bourbigot S, Le Bras M, Delobel R. Polymer International 1999;48: 264–70.
[23] Jimenez M, Duquesne S, Bourbigot S. Surface and Coatings Technology 2006; 201:979–87.
[24] Tuteja A, Duxbury PM, Mackay ME. Macromolecules 2007;40:9427–34.
[25] Wu K, Song L, Hu Y, Lu H, Kandola BK, Kandare E. Progress in Organic Coatings 2009;65:490–7.

Please cite this article in press as: Gérard C, et al., Reaction to fire of an intumescent epoxy resin: Protection mechanisms and synergy, Polymer Degradation and Stability (2012), doi:10.1016/j.polymdegradstab.2012.05.025